Transport theory up to second-order scattering for reaction-diffusion-phonon systems with applications to active transport in catalysis, explosions, and biological membranes

S. N. Patitsas ®*

Department of Physics & Astronomy, University of Lethbridge, 4401 University Drive, Lethbridge AB, Canada, T1K 3M4

A Boltzmann transport equation approach is developed for reaction-diffusion systems which incorporates phonon transport in addition to the traditional approach. Scattering processes up to second order are taken into account. Two forces emerge from this analysis when a spatial gradient exists, one force on reactants and products, the other force on phonons. The forces are equal and opposite and have the tendency for separation of the phonons away from the reactants and products. These forces are capable of creating the types of instabilities that can lead to the formation of Turing patterns. The existence of these forces allows for exergonic conversion where not all of the released energy from reactions and diffusion becomes heat. When applied to homogeneous catalysis, one finds that reactants and products are pushed toward regions of greater catalytic activity. In the realm of high-energy explosions, calculations show that reactants and products can be accelerated laterally to the direction of a TNT reaction front up to speeds near 1000 m/s. This acceleration is in opposition to diffusion and represents active transport. Calculations also show that active transport observed in biological systems such as bacteria, mitochondria, and chloroplasts may be explained by this second-order transport theory. Using reasonable values for key parameters, calculations show that up to one-third of the available chemical energy can be converted toward pumping protons uphill to a potential of 50 mV.

I. INTRODUCTION

Recent theoretical studies of electronic conduction at high currents has shown the existence of equal and opposite forces on electrons and phonons, if the system is inhomogeneous [1]. These forces are interesting because they are produced in a system that is otherwise merely dissipating energy. The approach uses a second-order transport equation built up by combining two Boltzmann transport equations, one for electrons and one for phonons. The predicted force pair can destabilize the dynamics for heat transfer. One such outcome is spontaneous symmetry breaking of the temperature field.

This approach has been adapted for use on reaction-diffusion systems and these results are presented here. The reaction part in particular adds complexity as more particles may partake, as compared to the electron-phonon case. An abundant amount of experimental and observational evidence is available for reaction-diffusion systems, including studies of reaction-diffusion Turing patterns [2,3]. Turing patterns are known to result from spontaneous symmetry breaking. It is of interest to the general scientific community to investigate if first principles transport theory can explain this pattern formation in detail.

It is also of interest to see if these results can be applied to biological systems that display the phenomenon of active transport. In active transport, particles are pushed uphill energetically, against the flow direction dictated by ordinary diffusion caused by a concentration gradient [4,5]. This type of particle transport is essential to the function of commonly found biological systems such as mitochondria, chloroplasts, and bacteria. Active transport is key to the chemiosmotic mechanism thought to play an important role in the energetics of biological systems. On this topic the goal is to ascertain whether or not any forces that might emerge from second-order transport in reaction-diffusion systems could be responsible for active transport.

Toward understanding the theoretical results presented here a common theme is to consider a purely dissipative system pushed away from thermodynamic equilibrium by some external agent which is then removed. Ordinarily then a certain amount of initial energy is dissipated away into the heat bath as the system returns to equilibrium. The existence of any new forces could change this outcome, and some of the energy may be diverted away from becoming heat.

For the electron-phonon case the system consisted of an electrical conductor and would normally be an open system connected to a source of both electromotive force and current. Here the thermodynamical reaction-diffusion system may be open or closed and consists of a set of reactant and product particles, undergoing both diffusion as well as reactions, either chemical or nuclear. The phonons, as well as the heat bath, are essentially built in.

In this discussion of reaction-diffusion, the particles making up the system will be treated using classical Maxwell-Boltzmann statistics, and are given the generic term of reaction-diffusion particles. These are not to be confused with the phonons which are massless, quantum, quasiparticles. The list of candidates for being reaction-diffusion particles is long, including atoms, ions, nuclei, molecules both small and large,

*steve.patitsas@uleth.ca

clusters, and includes the categories of reactants, products, and catalysts. The gradients in concentrations that produce diffusion will be treated as static or quasistatic and in this discussion should not be confused with the dynamical density undulations of the phonons (sound waves). Phonons in solids are well studied and phonon scattering plays an important role in nonequilibrium transport calculations of electrical conductivity in the solid state [6,7]. The specific phonon quasiparticles are not traditionally incorporated into studies of reaction-diffusion systems though [8–12]. Here they will play an important role, at the level of second-order scattering.

The theoretical approach presented here attempts to determine the dynamical equations for the concentrations $n_{\mathrm{rdp},i}(\mathbf{r}, t)$, with $i = A, B, C, ...$, of each type of reaction-diffusion particle $(A, B, C, ...)$ and well as the for the phonon density function $n_{\mathrm{ph}}(\mathbf{r}, t)$. This includes searching for any new and significant force terms which would directly affect the acceleration fields. One proven method for describing temporal changes to these fields caused by particle scattering is the Boltzmann transport equation. In this approach one focuses, for each reaction-diffusion particle, on the distribution function $g_{\mathbf{k},i}(\mathbf{r}, t)$, where $\mathbf{k}$ is the wave vector, as well as the distribution function for the phonons, $h_{\mathbf{q}}(\mathbf{r}, t)$, where $\mathbf{q}$ is the phonon wave vector. From the distribution functions, densities are easily obtained by summing over all wave vectors as $n_{\mathrm{rdp},i} = \int g_{\mathbf{k},i} d\mathbf{k}$ and $n_{\mathrm{ph}} = \int h_{\mathbf{q}} d\mathbf{q}$. Use of the Boltzmann transport formalism allows for careful accounting of the important temporal evolution terms for $g_{\mathbf{k},i}(\mathbf{r}, t)$ and $h_{\mathbf{q}}(\mathbf{r}, t)$, through the calculation of collision integrals, $\frac{\partial g_{\mathbf{k},i}}{\partial t}\big|_{\mathrm{coll}}$ and $\frac{\partial h_{\mathbf{q}}}{\partial t}\big|_{\mathrm{coll}}$. The microscopic transport approach taken here is a truncated approximation scheme under the BBGKY hierarchy [13] that couples the reaction-diffusion particle fields and phonon fields through a combination of the electron Boltzmann transport equation with the phonon Boltzmann transport equation [6,7,14–17]. This coupling demands a treatment up to second-order scattering. This first principles approach implemented here is capable of dealing with second-order scattering processes and leads to equations for the particle distribution dynamics, one for each type of particle. These equations will involve collision terms such as $\frac{\partial g_{\mathbf{k}}}{\partial t}\big|_{D2}$ for the case of reaction-diffusion particle diffusion at second-order scattering and $\frac{\partial g_{\mathbf{k}i}}{\partial t}\big|_{R2}$ (with $i = A, B, C, ...$) for the case of chemical reactions of reaction-diffusion particles, also at second order. The final step in the theoretical development is to account for spatial gradients which play a key role since the scattering events do not all occur at the same point in space.

The first-principles scattering calculations are presented for the case of pure diffusion in Sec. II, and the two reaction-diffusion-phonon Boltzmann transport equations are presented. Force terms are calculated at second order, including the force on the phonon field. Spatial gradients are then incorporated to produce a simple expression for the forces and potentials. A discussion for the energetics is included. A similar treatment is discussed in Sec. III for the case of reactions. After a discussion of simple combination reactions, the bimolecular reaction is considered, followed by a treatment of more general reactions. In Sec. IV, the general results are formulated into a theorem, with subsequent discussion. Afterwards, some example systems are considered and numerical

results are presented. In Sec. V, catalytic systems with spatial gradients are analyzed, followed by a study, in Sec. VI, of how the dynamics during explosions might be affected. Before concluding, a discussion of active transport in mitochondria and chloroplasts is made in Sec. VII.

II. CASE OF CONCENTRATION GRADIENTS AND DIFFUSION

Electron-phonon scattering has been well studied and the goal here is to take this system and adapt it to the case of reaction-diffusion. An electronic system that has been pushed away from equilibrium will, if allowed to, approach equilibrium via electron-phonon scattering and will create heat as it does so, i.e., Joule heating. A chemical system will also produce heat if pushed away from equilibrium on the exothermic side. In doing so, phonons must be created, and this can also be described by scattering processes.

To begin with, only one type of reaction-diffusion particle is treated, and reactions are not considered, only diffusion. One should think of a multicomponent system capable of multiple chemical reactions, but with all reaction channels somehow shut off, in this section only. All components may have concentration gradients, but to begin with, only one such component, or reaction-diffusion particle, is considered. The goal is to determine both the spatial variation as well as the time dependence of the local number density, $n_{\mathrm{rdp}}(\mathbf{r}, t)$ for this particle type. When this density is expressed in terms of the distribution function $g_{\mathbf{k}} \equiv g_{\mathbf{k}}(\mathbf{r}, t)$ as $n_{\mathrm{rdp}}(\mathbf{r}, t) = \int g_{\mathbf{k}} d\mathbf{k}$, then the problem is reduced to solving the Boltzmann transport equation:

$$\frac{\partial g_{\mathbf{k}}}{\partial t} + \mathbf{v} \cdot \frac{\partial g_{\mathbf{k}}}{\partial \mathbf{r}} + \frac{1}{\hbar}\mathbf{F}_{\mathrm{ext}} \cdot \frac{\partial g_{\mathbf{k}}}{\partial \mathbf{k}} = \frac{\partial g_{\mathbf{k}}}{\partial t}\bigg|_{\mathrm{coll}}, \quad (1)$$

where the velocity is $\mathbf{v} = \hbar\mathbf{k}/m$. The collision term is calculated here by accounting for first and second order in scattering, as will be discussed below:

$$\frac{\partial g_{\mathbf{k}}}{\partial t}\bigg|_{\mathrm{coll}} = \frac{\partial g_{\mathbf{k}}}{\partial t}\bigg|_{D1} + \frac{\partial g_{\mathbf{k}}}{\partial t}\bigg|_{D2}. \quad (2)$$

Focusing first on reaction-diffusion particle-phonon scattering at first order:

$$\frac{\partial g_{\mathbf{k}}}{\partial t}\bigg|_{D1} = \iint \{-g_{\mathbf{k}}(1 + h_{\mathbf{q}''}) + g_{\mathbf{k}'}h_{\mathbf{q}''}\}\mathcal{W}_{\mathbf{k}}^{\mathbf{k}',\mathbf{q}''}$$
$$\times \delta(\mathbf{k} - \mathbf{k}' - \mathbf{q}'')d\mathbf{k}'d\mathbf{q}'', \quad (3)$$

where $h_{\mathbf{q}}$ is the phonon distribution function for phonon wave vector $\mathbf{q}$, and $\mathcal{W}_{\mathbf{k}}^{\mathbf{k}',\mathbf{q}''}$ is the intrinsic transition probability and includes an energy conserving Dirac δ function [6]. For reaction-diffusion particle sums $d\mathbf{k} \equiv \frac{1}{8\pi^3}d^3\mathbf{k}$ while for phonons $d\mathbf{q} \equiv \frac{3}{8\pi^3}d^3\mathbf{q}$. These integrals are taken over the full momentum space. For example, q_x, q_y, and q_z all range from $-\infty$ to $+\infty$. The spin quantum numbers are suppressed in the notation here as no spin-dependence will be discussed. The distributions $g_{\mathbf{k}}$ and $h_{\mathbf{q}}$ are nonequilibrium in general. The equilibrium distributions are denoted as $g_{\mathbf{k}}^0$ and $h_{\mathbf{q}}^0$. Since classical Maxwell-Boltzmann statistics are used for the reaction-diffusion particles, $1 \pm g_{\mathbf{k}} \approx 1$ for outgoing

states. The first-order collision integral gives the traditional diffusion coefficient for the reaction-diffusion particles.

The second-order transport integrals for the electron-phonon system have been worked out previously [1]. This result is carried over with appropriate adaptation which is explained in detail below. Since electron flow is created by a gradient in electrochemical potential, the parallel with particle diffusion is clear. For the particular type of reaction-diffusion particle under consideration here, the important second-order collision integral is

$$
\begin{aligned}
\left.\frac{\partial g_{\boldsymbol{k}}}{\partial t}\right|_{D2} = \frac{1}{2} \int_0^\infty \iiiint &\Big[-g_{\boldsymbol{k}}(1+h_{\boldsymbol{q}''})\mathcal{W}_{\boldsymbol{k}}^{\boldsymbol{k}',\boldsymbol{q}''}\delta(\boldsymbol{k}-\boldsymbol{k}'-\boldsymbol{q}'')e^{-t'/\tau_{1,>}}h_{\boldsymbol{q}''}h_{\boldsymbol{q}}(1+h_{\boldsymbol{q}'})\mathcal{Q}_{\boldsymbol{q}'',\boldsymbol{q}}^{\boldsymbol{q}'}\delta(\boldsymbol{q}''+\boldsymbol{q}-\boldsymbol{q}') \\
&+ g_{\boldsymbol{k}'}h_{\boldsymbol{q}''}\mathcal{W}_{\boldsymbol{k}}^{\boldsymbol{k}',\boldsymbol{q}''}\delta(\boldsymbol{k}-\boldsymbol{k}'-\boldsymbol{q}'')e^{-t'/\tau_{1,<}}(1+h_{\boldsymbol{q}''})(1+h_{\boldsymbol{q}})h_{\boldsymbol{q}'}\mathcal{Q}_{\boldsymbol{q}'}^{\boldsymbol{q}'',\boldsymbol{q}}\delta(\boldsymbol{q}''+\boldsymbol{q}-\boldsymbol{q}') \\
&- g_{\boldsymbol{k}}(1+h_{\boldsymbol{q}''})\mathcal{W}_{\boldsymbol{k}}^{\boldsymbol{k}',\boldsymbol{q}''}\delta(\boldsymbol{k}-\boldsymbol{k}'-\boldsymbol{q}'')e^{-t'/\tau_{2,>}}h_{\boldsymbol{q}''}(1+h_{\boldsymbol{q}})(1+h_{\boldsymbol{q}'})\mathcal{Q}_{\boldsymbol{q}''}^{\boldsymbol{q},\boldsymbol{q}'}\delta(\boldsymbol{q}''-\boldsymbol{q}-\boldsymbol{q}') \\
&+ g_{\boldsymbol{k}'}h_{\boldsymbol{q}''}\mathcal{W}_{\boldsymbol{k}}^{\boldsymbol{k}',\boldsymbol{q}''}\delta(\boldsymbol{k}-\boldsymbol{k}'-\boldsymbol{q}'')e^{-t'/\tau_{2,<}}(1+h_{\boldsymbol{q}''})h_{\boldsymbol{q}}h_{\boldsymbol{q}'}\mathcal{Q}_{\boldsymbol{q},\boldsymbol{q}'}^{\boldsymbol{q}''}\delta(\boldsymbol{q}''-\boldsymbol{q}-\boldsymbol{q}')\Big]d\boldsymbol{k}'d\boldsymbol{q}d\boldsymbol{q}'d\boldsymbol{q}''dt',
\end{aligned}
\tag{4}
$$

In Eq. (4) one recognizes two scattering vertices, $\mathcal{W}_{\boldsymbol{k}}^{\boldsymbol{k}',\boldsymbol{q}''}$, as well as one for three-phonon scattering, $\mathcal{Q}_{\boldsymbol{q},\boldsymbol{q}'}^{\boldsymbol{q}''}$. For each vertex the explicit Dirac δ functions stipulate momentum conservation. The scattering diagrams illustrated in Fig. 1 help to understand the structure of the collision integral. The first line in Eq. (4) corresponds to Fig. 1(a), in which a reaction-diffusion particle with wave vector $\boldsymbol{k}$ scatters to produce $\boldsymbol{k}'$ at lower energy, and a virtual phonon $\boldsymbol{q}''$, which subsequently scatters with another phonon $\boldsymbol{q}$ to produce a final state phonon $\boldsymbol{q}'$. The right moving, >, virtual phonon has a lifetime $\tau_{1,>}$, hence the probabilistic factor $e^{-t'/\tau_{1,>}}$ along with integration over t' from 0 to ∞ [7]. Explicit dependence of this collision integral on the time t is contained in the distribution functions $g_{\boldsymbol{k}}(\mathbf{r},t)$, $g_{\boldsymbol{k}'}(\mathbf{r},t)$, $h_{\boldsymbol{q}}(\mathbf{r},t)$, $h_{\boldsymbol{q}'}(\mathbf{r},t)$, and $h_{\boldsymbol{q}''}(\mathbf{r},t)$. The second line in Eq. (4) [see Fig. 1(b)] corresponds to the time reversal of Fig. 1(a). The virtual phonon is left moving, <. Figures 1(c) and 1(d) form another time reversed pair. Apart from the possibility of 4-phonon processes this exhausts all possibilities. The manner of dealing with phonons is similar to Boltzmann transport calculations of thermal conductivity [6,17]. The second-order scattering approach taken here and depicted in Fig. 1 is not to be confused with what is more traditionally referred to as second-order transport theory which determines second-order corrections to particle distributions, while considering only one scattering vertex [18].

Pointing out symmetries such as $\mathcal{Q}_{\boldsymbol{q}'',\boldsymbol{q}}^{\boldsymbol{q}'} = \mathcal{Q}_{\boldsymbol{q}'}^{\boldsymbol{q}'',\boldsymbol{q}}$ and $\mathcal{Q}_{\boldsymbol{q}''}^{\boldsymbol{q},\boldsymbol{q}'} = \mathcal{Q}_{\boldsymbol{q},\boldsymbol{q}'}^{\boldsymbol{q}''}$ helps to simplify Eq. (4) as well as the following expressions for the complementary transport integrals:

$$
\begin{aligned}
\left.\frac{\partial g_{\boldsymbol{k}'}}{\partial t}\right|_{D2} = \frac{1}{2}\int_0^\infty \iiiint &\Big[\{e^{-t'/\tau_{1,>}}g_{\boldsymbol{k}}h_{\boldsymbol{q}}(1+h_{\boldsymbol{q}'}) - e^{-t'/\tau_{1,<}}g_{\boldsymbol{k}'}(1+h_{\boldsymbol{q}})h_{\boldsymbol{q}'}\}\mathcal{Q}_{\boldsymbol{q}'',\boldsymbol{q}}^{\boldsymbol{q}'}\delta(\boldsymbol{q}''+\boldsymbol{q}-\boldsymbol{q}') \\
&+ \{e^{-t'/\tau_{2,>}}g_{\boldsymbol{k}}(1+h_{\boldsymbol{q}})(1+h_{\boldsymbol{q}'}) - e^{-t'/\tau_{2,<}}g_{\boldsymbol{k}'}h_{\boldsymbol{q}}h_{\boldsymbol{q}'}\}\mathcal{Q}_{\boldsymbol{q}''}^{\boldsymbol{q},\boldsymbol{q}'}\delta(\boldsymbol{q}''-\boldsymbol{q}-\boldsymbol{q}')\Big] \\
&\times \mathcal{W}_{\boldsymbol{k}}^{\boldsymbol{k}',\boldsymbol{q}''}h_{\boldsymbol{q}''}(1+h_{\boldsymbol{q}''})\delta(\boldsymbol{k}-\boldsymbol{k}'-\boldsymbol{q}'')d\boldsymbol{k}d\boldsymbol{q}d\boldsymbol{q}'d\boldsymbol{q}''dt',
\end{aligned}
\tag{5}
$$

$$
\begin{aligned}
\left.\frac{\partial h_{\boldsymbol{q}}}{\partial t}\right|_{D2} = \int_0^\infty \iiiint &\Big[\{-e^{-t'/\tau_{1,>}}g_{\boldsymbol{k}}h_{\boldsymbol{q}}(1+h_{\boldsymbol{q}'}) + e^{-t'/\tau_{1,<}}g_{\boldsymbol{k}'}(1+h_{\boldsymbol{q}})h_{\boldsymbol{q}'}\}\mathcal{Q}_{\boldsymbol{q}'',\boldsymbol{q}}^{\boldsymbol{q}'}\delta(\boldsymbol{q}''+\boldsymbol{q}-\boldsymbol{q}') \\
&+ \{e^{-t'/\tau_{2,>}}g_{\boldsymbol{k}}(1+h_{\boldsymbol{q}})(1+h_{\boldsymbol{q}'}) - e^{-t'/\tau_{2,<}}g_{\boldsymbol{k}'}h_{\boldsymbol{q}}h_{\boldsymbol{q}'}\}\mathcal{Q}_{\boldsymbol{q}''}^{\boldsymbol{q},\boldsymbol{q}'}\delta(\boldsymbol{q}''-\boldsymbol{q}-\boldsymbol{q}')\Big] \\
&\times \mathcal{W}_{\boldsymbol{k}}^{\boldsymbol{k}',\boldsymbol{q}''}h_{\boldsymbol{q}''}(1+h_{\boldsymbol{q}''})\delta(\boldsymbol{k}-\boldsymbol{k}'-\boldsymbol{q}'')d\boldsymbol{k}d\boldsymbol{k}'d\boldsymbol{q}'d\boldsymbol{q}''dt',
\end{aligned}
\tag{6}
$$

$$
\begin{aligned}
\left.\frac{\partial h_{\boldsymbol{q}'}}{\partial t}\right|_{D2} = \int_0^\infty \iiiint &\Big[\{e^{-t'/\tau_{1,>}}g_{\boldsymbol{k}}h_{\boldsymbol{q}}(1+h_{\boldsymbol{q}'}) - e^{-t'/\tau_{1,<}}g_{\boldsymbol{k}'}(1+h_{\boldsymbol{q}})h_{\boldsymbol{q}'}\}\mathcal{Q}_{\boldsymbol{q}'',\boldsymbol{q}}^{\boldsymbol{q}'}\delta(\boldsymbol{q}''+\boldsymbol{q}-\boldsymbol{q}') \\
&+ \{e^{-t'/\tau_{2,>}}g_{\boldsymbol{k}}(1+h_{\boldsymbol{q}})(1+h_{\boldsymbol{q}'}) - e^{-t'/\tau_{2,<}}g_{\boldsymbol{k}'}h_{\boldsymbol{q}}h_{\boldsymbol{q}'}\}\mathcal{Q}_{\boldsymbol{q}''}^{\boldsymbol{q},\boldsymbol{q}'}\delta(\boldsymbol{q}''-\boldsymbol{q}-\boldsymbol{q}')\Big] \\
&\times \mathcal{W}_{\boldsymbol{k}}^{\boldsymbol{k}',\boldsymbol{q}''}h_{\boldsymbol{q}''}(1+h_{\boldsymbol{q}''})\delta(\boldsymbol{k}-\boldsymbol{k}'-\boldsymbol{q}'')d\boldsymbol{k}d\boldsymbol{k}'d\boldsymbol{q}d\boldsymbol{q}''dt'.
\end{aligned}
\tag{7}
$$

Still, these expressions remain rather complicated when compared to the first-order collision integrals. The collision terms in Eqs. (6) and (7) affect the spatial and temporal dependencies of the phonon density field and therefore the temperature field. These collision terms are incorporated into the standard phonon Boltzmann transport equation:

$$
\frac{\partial h_{\boldsymbol{q}}}{\partial t} + \boldsymbol{c}_{\boldsymbol{q}}\cdot\nabla\mathrm{T}\frac{\partial h_{\boldsymbol{q}}}{\partial T} = \left.\frac{\partial h_{\boldsymbol{q}}}{\partial t}\right|_{D1} + \left.\frac{\partial h_{\boldsymbol{q}}}{\partial t}\right|_{D2},
\tag{8}
$$

which involves the temperature field $T(\mathbf{r},t)$, and the phonon velocity $\boldsymbol{c}_{\boldsymbol{q}}$ [17]. Equation (8), along with Eq. (1) for the reaction-diffusion particle distribution, constitute the reaction-diffusion-phonon Boltzmann transport equations.

A. Summary of first-order scattering results (single vertex)

Given the extra complications of second-order scattering theory, as compared to first order, it is helpful to introduce
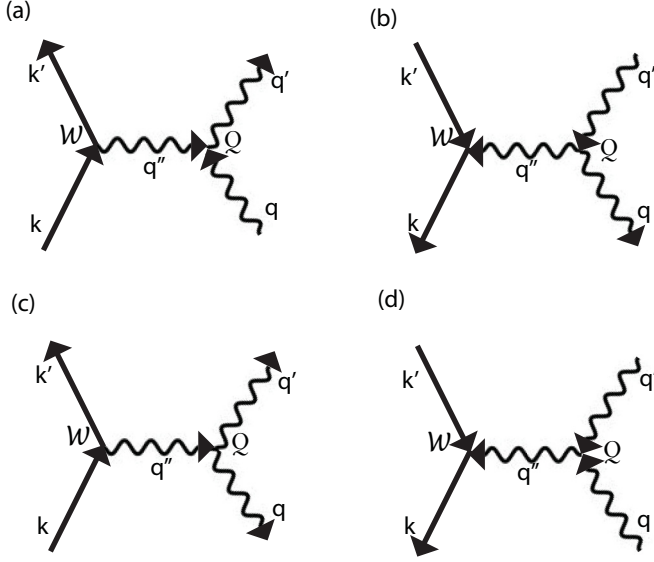
FIG. 1. Second-order reaction-diffusion particle-phonon scattering diagrams, for diffusion, covering all cases with three-phonon scattering. Two vertices are present, labeled $\mathcal{W}$ for reaction-diffusion particle-phonon and $\mathcal{Q}$ for phonon-phonon interaction.

some first-order quantities and use these to help understand and factorize the second-order theory. From Eq. (3), the phonon scattering rate for reaction-diffusion particles may be expressed as

$$
\begin{aligned}
\frac{1}{\tau_{\text{rdp}}} &= -\frac{1}{n_{\text{rdp}}}\int \frac{\partial g_k}{\partial t}\bigg|_{D1} d\boldsymbol{k} \\
&= \frac{1}{n_{\text{rdp}}}\iiint \{g_{\boldsymbol{k}}(1+h_{q''}) - g_{\boldsymbol{k}'}h_{q''}\}\mathcal{W}_{\boldsymbol{k}}^{\boldsymbol{k}',\boldsymbol{q}''} \\
&\quad \times \delta(\boldsymbol{k}-\boldsymbol{k}'-\boldsymbol{q}'')d\boldsymbol{k}d\boldsymbol{k}'d\boldsymbol{q}''.
\end{aligned} \tag{9}
$$

Also, the rate at which energy is transferred from reaction-diffusion particles to phonons by diffusion is

$$
\begin{aligned}
\dot{u}_D &= \iiint \varepsilon_{q''}\{g_{\boldsymbol{k}}(1+h_{q''}) - g_{\boldsymbol{k}'}h_{q''}\}\mathcal{W}_{\boldsymbol{k}}^{\boldsymbol{k}',\boldsymbol{q}''} \\
&\quad \times \delta(\boldsymbol{k}-\boldsymbol{k}'-\boldsymbol{q}'')d\boldsymbol{k}d\boldsymbol{k}'d\boldsymbol{q}''.
\end{aligned} \tag{10}
$$

In terms of the dissipation rate, $\dot{u}_D$, a type of mean phonon energy is defined as

$$
\bar{\varepsilon} \equiv \dot{u}_D\,\tau_{\text{rdp}}/n_{\text{rdp}}. \tag{11}
$$

In Eq. (10), one identifies a positive production rate (forward flow) counteracted by the back flow term with the minus sign. Under conditions of very steep density gradients, the forward

flow term will greatly exceed the back flow term. The energy stored in the phonon field, $U = \int u\,dV$ plays an important role in this analysis. It represents the energy of the heat bath which increases as the nonequilibrium systems considered here approach equilibrium.

In Appendix A it is shown that for a near equilibrium system of reaction-diffusion particles with mass m, number density, n_{rdp}, and current density J:

$$
\begin{aligned}
\dot{u}_D &= \frac{2}{3}\beta^2 K \iiint g_k^0(1+h_{q''}^0)\mathcal{W}_{\boldsymbol{k}}^{\boldsymbol{k}',\boldsymbol{q}''} \\
&\quad \times \delta(\boldsymbol{k}-\boldsymbol{k}'-\boldsymbol{q}'')\varepsilon_{q''}^2 d\boldsymbol{k}d\boldsymbol{k}'d\boldsymbol{q}'',
\end{aligned} \tag{12}
$$

where

$$
K = \frac{mJ^2}{2n_{\text{rdp}}^2}, \tag{13}
$$

is the per particle kinetic energy of the drift.

Focusing on a single three-phonon vertex, first-order theory gives:

$$
\frac{1}{\tau_{1,>}'} \equiv \frac{1}{2}\iint h_q(1+h_{q'})h_{q''}\mathcal{Q}_{q'',q}^{q'}\delta(\boldsymbol{q}''+\boldsymbol{q}-\boldsymbol{q}')d\boldsymbol{q}d\boldsymbol{q}', \tag{14}
$$

$$
\frac{1}{\tau_{1,<}'} \equiv \frac{1}{2}\iint (1+h_q)h_{q'}(1+h_{q''})\mathcal{Q}_{q'',q}^{q'}\delta(\boldsymbol{q}''+\boldsymbol{q}-\boldsymbol{q}')d\boldsymbol{q}d\boldsymbol{q}', \tag{15}
$$

$$
\frac{1}{\tau_{2,>}'} \equiv \frac{1}{2}\iint (1+h_q)(1+h_{q'})h_{q''}\mathcal{Q}_{q''}^{q,q'}\delta(\boldsymbol{q}''-\boldsymbol{q}-\boldsymbol{q}')d\boldsymbol{q}d\boldsymbol{q}', \tag{16}
$$

$$
\frac{1}{\tau_{2,<}'} \equiv \frac{1}{2}\iint h_q h_{q'}(1+h_{q''})\mathcal{Q}_{q''}^{q,q'}\delta(\boldsymbol{q}''-\boldsymbol{q}-\boldsymbol{q}')d\boldsymbol{q}d\boldsymbol{q}'. \tag{17}
$$

Note in these expressions the times are primed. The reason for this will become clear below as the primed and unprimed times are not to be calculated at the same point in space.

With these definitions one can return to the second-order collision integrals and rewrite Eq. (4) as

$$
\begin{aligned}
\frac{\partial g_k}{\partial t}\bigg|_{D2} &= -\int_0^\infty \iint \bigg[e^{-t'/\tau_{1,>}} g_{\boldsymbol{k}}(1+h_{q''})\frac{1}{\tau_{1,>}'} \\
&\quad - e^{-t'/\tau_{1,<}} g_{\boldsymbol{k}'}h_{q''}\frac{1}{\tau_{1,<}'} + e^{-t'/\tau_{2,>}} g_{\boldsymbol{k}}(1+h_{q''})\frac{1}{\tau_{2,>}'} \\
&\quad - e^{-t'/\tau_{2,<}} g_{\boldsymbol{k}'}h_{q''}\frac{1}{\tau_{2,<}'} \bigg]\mathcal{W}_{\boldsymbol{k}}^{\boldsymbol{k}',\boldsymbol{q}''} \\
&\quad \times \delta(\boldsymbol{k}-\boldsymbol{k}'-\boldsymbol{q}'')d\boldsymbol{k}'d\boldsymbol{q}''dt'.
\end{aligned} \tag{18}
$$

B. Force terms for phonons and reaction-diffusion particles

Returning to second-order scattering theory and Eqs. (4) and (5), for the reaction-diffusion particles, the force per unit volume from such collisions is given by

$$
\boldsymbol{f}_{\text{rdp},D} = \hbar \int \frac{\partial g_k}{\partial t}\bigg|_{D2} \boldsymbol{k}\,d\boldsymbol{k} + \hbar \int \frac{\partial g_{k'}}{\partial t}\bigg|_{D2} \boldsymbol{k}'\,d\boldsymbol{k}'. \tag{19}
$$

This force is added in with any other contributions to the rate of change of reaction-diffusion particle momentum density, $\partial \boldsymbol{p}_{\mathrm{rdp}}/\partial t$. Noting that $\boldsymbol{q}'' = \boldsymbol{k} - \boldsymbol{k}'$,

$$
\boldsymbol{f}_{\mathrm{rdp},D} = -\hbar \int_0^\infty \iiint \boldsymbol{q}'' \left[e^{-t'/\tau_{1,>}} g_{\boldsymbol{k}}(1 + h_{\boldsymbol{q}''}) \frac{1}{\tau_{1,>}'} - e^{-t'/\tau_{1,<}} g_{\boldsymbol{k}'} h_{\boldsymbol{q}''} \frac{1}{\tau_{1,<}'} \right.
$$
$$
\left. + e^{-t'/\tau_{2,>}} g_{\boldsymbol{k}}(1 + h_{\boldsymbol{q}''}) \frac{1}{\tau_{2,>}'} - e^{-t'/\tau_{2,<}} g_{\boldsymbol{k}} h_{\boldsymbol{q}''} \frac{1}{\tau_{2,<}'} \right] \mathcal{W}_{\boldsymbol{k}}^{\boldsymbol{k}',\boldsymbol{q}''} \delta(\boldsymbol{k} - \boldsymbol{k}' - \boldsymbol{q}'') d\boldsymbol{k} d\boldsymbol{k}' d\boldsymbol{q}'' dt'. \tag{20}
$$

For completeness, the force on the phonon field can be calculated independently as

$$
\boldsymbol{f}_{p,D} = \frac{1}{2} \hbar \int \left. \frac{\partial h_q}{\partial t} \right|_{D2} \boldsymbol{q} \, dq + \frac{1}{2} \hbar \int \left. \frac{\partial h_{q'}}{\partial t} \right|_{D2} \boldsymbol{q}' \, dq'. \tag{21}
$$

By Eqs. (6) and (7),

$$
\boldsymbol{f}_{p,D} = \frac{\hbar}{2} \int_0^\infty \iiiint \left[\{ -e^{-t'/\tau_{1,>}} g_{\boldsymbol{k}} h_q (1 + h_{q'}) + e^{-t'/\tau_{1,<}} g_{\boldsymbol{k}'}(1 + h_q) h_{q'} \} \mathcal{Q}_{\boldsymbol{q}'',q}^{q'} \delta(\boldsymbol{q}'' + \boldsymbol{q} - \boldsymbol{q}') \boldsymbol{q} \right.
$$
$$
\left. + \{ e^{-t'/\tau_{2,>}} g_{\boldsymbol{k}}(1 + h_q)(1 + h_{q'}) - e^{-t'/\tau_{2,<}} g_{\boldsymbol{k}'} h_q h_{q'} \} \mathcal{Q}_{\boldsymbol{q}''}^{q,q'} \delta(\boldsymbol{q}'' - \boldsymbol{q} - \boldsymbol{q}') \boldsymbol{q} \right]
$$
$$
\times \mathcal{W}_{\boldsymbol{k}}^{\boldsymbol{k}',\boldsymbol{q}''} h_{\boldsymbol{q}''}(1 + h_{\boldsymbol{q}''}) \delta(\boldsymbol{k} - \boldsymbol{k}' - \boldsymbol{q}'') d\boldsymbol{k} d\boldsymbol{k}' d\boldsymbol{q} d\boldsymbol{q}' d\boldsymbol{q}'' dt'
$$
$$
+ \frac{\hbar}{2} \int_0^\infty \iiiint \left[\{ e^{-t'/\tau_{1,>}} g_{\boldsymbol{k}} h_q (1 + h_{q'}) - e^{-t'/\tau_{1,<}} g_{\boldsymbol{k}'}(1 + h_q) h_{q'} \} \mathcal{Q}_{\boldsymbol{q}'',q}^{q'} \delta(\boldsymbol{q}'' + \boldsymbol{q} - \boldsymbol{q}') \boldsymbol{q}' \right.
$$
$$
\left. + \{ e^{-t'/\tau_{2,>}} g_{\boldsymbol{k}}(1 + h_q)(1 + h_{q'}) - e^{-t'/\tau_{2,<}} g_{\boldsymbol{k}'} h_q h_{q'} \} \mathcal{Q}_{\boldsymbol{q}''}^{q,q'} \delta(\boldsymbol{q}'' - \boldsymbol{q} - \boldsymbol{q}') \boldsymbol{q}' \right]
$$
$$
\times \mathcal{W}_{\boldsymbol{k}}^{\boldsymbol{k}',\boldsymbol{q}''} h_{\boldsymbol{q}''}(1 + h_{\boldsymbol{q}''}) \delta(\boldsymbol{k} - \boldsymbol{k}' - \boldsymbol{q}'') d\boldsymbol{k} d\boldsymbol{k}' d\boldsymbol{q} d\boldsymbol{q}' d\boldsymbol{q}'' dt'. \tag{22}
$$

Using $\boldsymbol{q}' - \boldsymbol{q} = \boldsymbol{q}''$ in the first and fourth rows, and $\boldsymbol{q}' + \boldsymbol{q} = \boldsymbol{q}''$ in the second and fifth rows results in

$$
\boldsymbol{f}_{p,D} = \frac{\hbar}{2} \int_0^\infty \iiiint \left[\{ e^{-t'/\tau_{1,>}} g_{\boldsymbol{k}} h_q (1 + h_{q'}) - e^{-t'/\tau_{1,<}} g_{\boldsymbol{k}'}(1 + h_q) h_{q'} \} \mathcal{Q}_{\boldsymbol{q}'',q}^{q'} \delta(\boldsymbol{q}'' + \boldsymbol{q} - \boldsymbol{q}') \boldsymbol{q}'' \right.
$$
$$
\left. + \{ e^{-t'/\tau_{2,>}} g_{\boldsymbol{k}}(1 + h_q)(1 + h_{q'}) - e^{-t'/\tau_{2,<}} g_{\boldsymbol{k}'} h_q h_{q'} \} \mathcal{Q}_{\boldsymbol{q}''}^{q,q'} \delta(\boldsymbol{q}'' - \boldsymbol{q} - \boldsymbol{q}') \boldsymbol{q}'' \right]
$$
$$
\times \mathcal{W}_{\boldsymbol{k}}^{\boldsymbol{k}',\boldsymbol{q}''} h_{\boldsymbol{q}''}(1 + h_{\boldsymbol{q}''}) \delta(\boldsymbol{k} - \boldsymbol{k}' - \boldsymbol{q}'') d\boldsymbol{k} d\boldsymbol{k}' d\boldsymbol{q} d\boldsymbol{q}' d\boldsymbol{q}'' dt'. \tag{23}
$$

With this form, Eqs. (14), (15), (16), and (17) can be invoked and the result compared to Eq. (20) to show the important result

$$
\boldsymbol{f}_{p,D} = -\boldsymbol{f}_{\mathrm{rdp},D}. \tag{24}
$$

This simple result, resembling Newton's third law of action-reaction, guarantees momentum conservation. For second-order reaction-diffusion particle-phonon scattering, a force pair exists much like for the case of second-order electron-phonon scattering [1].

C. Spatial variation in the transition rate

The factor of $\boldsymbol{q}''$ in Eq. (20) will make the integral zero by symmetry unless there is some spatial variation, for example in the matrix element $\mathcal{W}_{\boldsymbol{k}}^{\boldsymbol{k}',\boldsymbol{q}''}$. The same is true if the occupation factors $g_{\boldsymbol{k}}$, $g_{\boldsymbol{k}'}$, $h_{\boldsymbol{q}''}$ as well as the rates $1/\tau_{\boldsymbol{q}''}$ vary spatially. Here $\tau_{\boldsymbol{q}''}$ refers to any one of $\tau_{1,>}$, $\tau_{1,<}$, $\tau_{2,>}$, or $\tau_{2,<}$. Note the two scattering vertices do not occur at the same time and place. A simple approach is taken here to deal with the spatial variations which is qualitatively similar to textbook treatments of first-order transport physics [7,19]. The temporal separation between the two scattering vertices is $\tau_{\boldsymbol{q}''}$ and the spatial separation is $c\tau_{\boldsymbol{q}''}$ where c is the phonon speed. If $\boldsymbol{r}$ is the location of the midpoint of the line segment joining the reaction-diffusion particle-phonon collision to the three-phonon collision, then

$\mathcal{W}_{\boldsymbol{k}}^{\boldsymbol{k}',\boldsymbol{q}''}$ must be evaluated at $\boldsymbol{r} - \Delta\boldsymbol{r}$ where $\Delta\boldsymbol{r} = \frac{1}{2} c\tau_{\boldsymbol{q}''}\hat{\boldsymbol{q}}''$ and $\hat{\boldsymbol{q}}'' = \boldsymbol{q}''/q''$. So also must $g_{\boldsymbol{k}}$, $g_{\boldsymbol{k}'}$, and $h_{\boldsymbol{q}''}$ be evaluated at $\boldsymbol{r} - \Delta\boldsymbol{r}$. In contrast, since the lifetime $\tau_{\boldsymbol{q}''}$ involves phonon-phonon scattering with vertex $\mathcal{Q}_{\boldsymbol{q}''}^{q,q'}$, it must be evaluated at position $\boldsymbol{r} + \Delta\boldsymbol{r}$. Note the $\tau_{\boldsymbol{q}''}$ in the exponents in Eq. (20) are calculated at $\boldsymbol{r}$.

Taylor expansions are taken up to first order. Focusing on the first of the four terms in Eq. (20):

$$
g_{\boldsymbol{k}}(1 + h_{\boldsymbol{q}''})\mathcal{W}_{\boldsymbol{k}}^{\boldsymbol{k}',\boldsymbol{q}''}\big|_{\boldsymbol{r}-\Delta\boldsymbol{r}} = g_{\boldsymbol{k}}(1 + h_{\boldsymbol{q}''})\mathcal{W}_{\boldsymbol{k}}^{\boldsymbol{k}',\boldsymbol{q}''}\big|_{\boldsymbol{r}}
$$
$$
- \Delta\boldsymbol{r} \cdot \nabla \big[g_{\boldsymbol{k}}(1 + h_{\boldsymbol{q}''})\mathcal{W}_{\boldsymbol{k}}^{\boldsymbol{k}',\boldsymbol{q}''} \big]. \tag{25}
$$

Also

$$
\frac{1}{\tau_{1,>}'} = \frac{1}{\tau_{1,>}}\bigg|_{\boldsymbol{r}+\Delta\boldsymbol{r}} = \frac{1}{\tau_{1,>}} - \frac{1}{\tau_{1,>}^2}\Delta\boldsymbol{r} \cdot \nabla\tau_{1,>}. \tag{26}
$$

Multiplying Eqs. (25) and (26) gives a leading term, $g_{\boldsymbol{k}}(1 + h_{\boldsymbol{q}''})\mathcal{W}_{\boldsymbol{k}}^{\boldsymbol{k}',\boldsymbol{q}''}/\tau_{1,>}$, that will integrate to zero, and two terms first order in $\Delta\boldsymbol{r}$. These two terms are combined using the product rule to give the factor

$$
-\frac{1}{\tau_{1,>}^2}\Delta\boldsymbol{r} \cdot \nabla \big[g_{\boldsymbol{k}}(1 + h_{\boldsymbol{q}''})\mathcal{W}_{\boldsymbol{k}}^{\boldsymbol{k}',\boldsymbol{q}''}\tau_{1,>} \big], \tag{27}
$$

which is reinserted into Eq. (20) to give for the first of four force terms:

$$f_{\text{rdp},1} = \hbar \int_0^\infty \iiint \frac{e^{-t'/\tau_{1,>}}}{\tau_{1,>}^2} \Delta r \cdot \nabla \left[g_k (1 + h_{q''}) \mathcal{W}_k^{k',q''} \tau_{1,>} \right]$$
$$\times \, \delta(k - k' - q'') q'' dk dk' dq'' dt'. \tag{28}$$

Completing the time integral,

$$f_{\text{rdp},1} = \frac{1}{2} \iiint \varepsilon_{q''} \left\{ \hat{q}'' \cdot \nabla \left[g_k (1 + h_{q''}) \mathcal{W}_k^{k',\hat{q}''} \tau_{1,>} \right] \right\}$$
$$\times \, \delta(k - k' - q'') \hat{q}'' dk dk' dq'', \tag{29}$$

where $\varepsilon_{q''} = \hbar c q''$ is the dispersion relation for the virtual phonon. For large phonon frequencies, the dispersion relation may not be linear; The group velocity then becomes small and Eq. (29) will overestimate the force. Indeed, even if optical phonon modes exist, their contribution to $f_{\text{rdp},1}$ will be small. Thus, it is understood that the low to mid-range frequency acoustic phonons will make the major contributions to these forces. Note that since these lower frequency acoustic phonons have relatively longer lifetimes, the mean lifetime, τ^*, as calculated below, may be longer than if calculated other ways. For systems with high symmetry (gas, liquid phases, cubic) any term containing a factor of $q_i q_j$, $i \neq j$, give zero, and thus

$$f_{\text{rdp},1} = \frac{1}{6} \nabla \iiint \varepsilon_{q''} g_k (1 + h_{q''}) \mathcal{W}_k^{k',q''} \tau_{1,>}$$
$$\times \, \delta(k - k' - q'') dk dk' dq''. \tag{30}$$

In Eq. (30) any spatial variation in $\varepsilon_{q''}$ has been neglected.

The analysis for the second, term is similar, though the direction of Δr must be reversed since the virtual phonon q'' travels from the $\mathcal{Q}_{q'',q}^{q'}$ vertex to the $\mathcal{W}_k^{k',q''}$ vertex in this case. Accounting for this extra minus sign gives

$$f_{\text{rdp},2} = \frac{1}{6} \nabla \iiint \varepsilon_{q''} g_{k'} h_{q''} \mathcal{W}_k^{k',q''} \tau_{1,<}$$
$$\times \, \delta(k - k' - q'') dk dk' dq''. \tag{31}$$

Defining $\tau_> \equiv \frac{1}{2}(\tau_{1,>} + \tau_{2,>})$ and $\tau_< \equiv \frac{1}{2}(\tau_{1,<} + \tau_{2,<})$ one deals with all four terms, thus giving

$$f_{\text{rdp},D} = \frac{1}{3} \nabla \iiint \varepsilon_{q''} [g_k (1 + h_{q''}) \tau_> + g_{k'} h_{q''} \tau_<] \mathcal{W}_k^{k',q''}$$
$$\times \, \delta(k - k' - q'') dk dk' dq''. \tag{32}$$

D. Discussion of system near equilibrium

In local equilibrium, the principle of detailed balance dictates that

$$g_k^0 (1 + h_{q'}^0) = g_{k'}^0 h_{q'}^0, \tag{33}$$

as well as

$$h_q^0 (1 + h_{q'}^0) h_{q''}^0 = (1 + h_q^0) h_{q'}^0 (1 + h_{q''}^0), \tag{34}$$

and

$$h_q^0 h_{q'}^0 (1 + h_{q''}^0) = (1 + h_q^0)(1 + h_{q'}^0) h_{q''}^0. \tag{35}$$

By Eqs. (14), (15), (16), and (17), $\tau_{1,>}^0 = \tau_{1,<}^0$ and $\tau_{2,>}^0 = \tau_{2,<}^0$. Thus,

$$g_k^0 (1 + h_{q'}^0) \tau_>^0 - g_{k'}^0 h_{q'}^0 \tau_<^0 = 0. \tag{36}$$

This means, for example, that in local equilibrium the net rate of energy transfer to phonons is zero, i.e., $\dot{u}_{p,D} = 0$ according to Eq. (10); the forward flow and back flow exactly cancel.

Equation (36) differs by a minus sign from what is found in the integrand of Eq. (32) for the force when evaluated in local equilibrium. This peculiar result is caused by the extra minus sign in the back flow term as mentioned above for the derivation of Eq. (31). Given that the force on the phonons is equal and opposite, the physical significance may be that the reaction-diffusion particles become separated from the phonons, a type of matter-energy separation. If so, then this type of relaxation is indicative of an instability, similar to Peierls distortion as well as to the charge-spin separation that occurs in one-dimensional systems [20–22]. The system would relax until the forces f_{rdp} and f_p are balanced.

It may be that inclusion of scattering terms at third order and higher would rectify this issue. Taking into account more scattering vertices beyond any of the Q vertices in Fig. 1 should give more accurate calculation of the scattering rates $\tau_{1,>}^{-1}$, $\tau_{1,<}^{-1}$, $\tau_{2,>}^{-1}$, and $\tau_{2,<}^{-1}$. To lowest order these were defined in Eqs. (14), (15), (16), and (17). Adding more vertices then would only result in more accurate versions of $\tau_>$ and $\tau_<$ in Eq. (32), but the force will still be nonzero in local equilibrium.

Further study on this point is warranted. Future studies of such second- (and higher-) order scattering calculations must be carried out with great care in regards to how spatial gradients are treated. If, after further study, it turns out that these forces are simply not possible in local equilibrium, then an explanation may come from taking a more sophisticated approach, perhaps similar to the Fokker-Planck equation approach taken by van Kampen when he analyzed the current flowing through a nonlinear semiconducting p-n junction rectifier [23]. It may be that the distributions used here are too simplistic and that a more careful analysis will produce $f_{\text{rdp}} = 0$ in thermodynamic (local) equilibrium. If so, then simply reversing the sign of $g_{k'} h_{q''} \tau_<$ in Eq. (32) would indeed force $f_{\text{rdp}} = 0$ at local equilibrium, and may produce a good approximation near local equilibrium, but that is as far as one can go with the approach taken here. A variational, perturbative approach may also be used to force $f_{\text{rdp}} = 0$ at equilibrium [18,19]. An approach based more on fundamental quantum mechanics may also yield insights into this issue. For example, if a second-order extension of the recently developed Wigner transport equation is developed, then it may be well suited for dealing with the phonon wave functions and would not suffer from the abruptness of creation and annihilation present in the above analysis [24].

For systems under local equilibrium only, there may be no good reason to expect these forces to be zero. For example, if a temperature gradient exists, then there will be a gradient in $h_{q''}$ and therefore a nonzero f_{rdp} is expected. In this case the system is not in global equilibrium and there may not be anything peculiar about a nonzero f_{rdp}. If, however, it is $\mathcal{W}_k^{k',q''}$ that varies spatially, then it is conceivable to

have thermodynamic equilibrium holding globally. A good example for the electron-phonon case is an interface between two materials of different conductivity, where $\mathcal{W}_k^{k',q''}$ changes abruptly near the interface. Differences in chemical potential are balanced by electric fields after charge redistribution to achieve equilibrium. Adding f_{rdp} will shift this equilibrium by an extra electric field via F_{ext} in Eq. (1). Technically speaking, an interface may not be true equilibrium since over very long timescales the two materials will intermix and remove the gradient in $\mathcal{W}_k^{k',q''}$. The same argument holds for the example of biological membranes to be discussed below. However, for the much shorter timescales of interest to the research community, this technicality may be ignored, the heterostructures may be assumed to exist indefinitely, and thermodynamic equilibrium may be understood to hold globally in such heterogeneous systems. Thus, it does indeed appear that a nonzero f_{rdp} can exist under equilibrium conditions.

In any case, more detailed analysis near equilibrium will be left for future study and for the remainder of this paper, the pragmatic choice is taken to focus on conditions well away from local equilibrium. Under these conditions the back flow terms are relatively small and may be safely ignored. The same approach is taken below for chemical reactions with the forward, exothermic, direction taking precedence over the back-reaction. This is analogous to how the reverse current term is often dropped in Shockley's equation for the electrical current in a semiconductor p-n junction under typical forward bias operating conditions [7].

E. Well away from local equilibrium

When the system under study is well away from local equilibrium, the rate of energy dissipation is high, but not so high as to cause permanent change to the system, even after many cycles. Neglecting the back flow terms leaves, to a good approximation:

$$f_{\mathrm{rdp},D} = -\nabla w_D, \qquad (37)$$

where

$$w_D = -\frac{1}{3}\iiint \tau_> g_k (1 + h_{q''})\mathcal{W}_k^{k',q''}$$
$$\times \delta(k - k' - q'')\varepsilon_{q''} dk\,dk'\,dq'', \qquad (38)$$

which has the dimensions of energy density and acts as a potential for the reaction-diffusion particles. The integral on the right-hand side of Eq. (38) is not spatially uniform in general. That the forces $f_{\mathrm{rdp},D}$ and $f_{p,D}$ add up to zero is not surprising. This is just a statement of conservation of momentum. What is surprising is that each of the forces is not zero in general.

Noting the similarity between Eqs. (10) and (38), one defines

$$\tau^* \equiv \frac{\iiint \tau_> g_k (1 + h_{q''})\mathcal{W}_k^{k',q''}\delta(k - k' - q'')\varepsilon_{q''} dk\,dk'\,dq''}{\iiint g_k (1 + h_{q''})\mathcal{W}_k^{k',q''}\delta(k - k' - q'')\varepsilon_{q''} dk\,dk'\,dq''}, \qquad (39)$$

as a type of nonequilibrium mean value of the phonon lifetime $\tau_>$. The definition, Eq. (39) for τ^* allows one to write the

potential energy w_D in terms of the dissipation rate as

$$w_D = -\frac{1}{3}\tau^* \dot{u}_D. \qquad (40)$$

The value of τ^* will depend on the conditions that send the system out of equilibrium. Nevertheless, a good approximation would be expected by evaluating g_k and $h_{q''}$ in local equilibrium. Indeed, using the near equilibrium approximation implemented in Appendix A gives a prefactor $\frac{2}{3}\beta^2 K$ as found in Eq. (12). This prefactor appears in both numerator and denominator of Eq. (39) and cancels, leaving, to a good approximation,

$$\tau^* = \frac{\iiint \tau_> g_k^0 (1 + h_{q''}^0)\mathcal{W}_k^{k',q''}\delta(k - k' - q'')\varepsilon_{q''} dk\,dk'\,dq''}{\iiint g_k^0 (1 + h_{q''}^0)\mathcal{W}_k^{k',q''}\delta(k - k' - q'')\varepsilon_{q''} dk\,dk'\,dq''}. \qquad (41)$$

If βK is not small compared to unity, then correction terms will be needed, but again, these exist on both top and bottom and will cancel. If $\tau_>$ varies with phonon energy $\varepsilon_{q''}$, then an extra term appears for the numerator only. This term competes with βK though, and should only provide small corrections. As an example of this variation, phonon lifetimes are expected to be shorter for optical phonons than for acoustic phonons. For systems pushed well away from equilibrium via g_k, these variations in phonon lifetime will have only small effects on τ^*.

Also noteworthy is the presence of $\mathcal{W}_k^{k',q''}$ in both numerator and denominator. The integration over all available wave vectors will have a tendency to wash out any functional structure, and therefore to have the effects of $\mathcal{W}_k^{k',q''}$ on the numerator getting canceled by the same effects in the denominator. If one imagines another type of reaction-diffusion particle with a different $\mathcal{W}_k^{k',q''}$ (perhaps significantly larger), then it is still expected to have a similar value of τ^*. This reasoning leads to the following useful rule:

Rule for τ^*:
The virtual phonon mean lifetime τ^*, as defined by Eq. (39), is approximately independent of the specific reaction-diffusion particle and the conditions involved in creating the virtual phonon.

In the more complicated systems discussed below, there will be more than one τ^* and this rule may be invoked to aid in practical calculations, by assuming the τ^*s are all the same.

F. Effect on phonon field

The force on the phonon field is

$$f_{p,D} = -f_{\mathrm{rdp},D} = \nabla w_D. \qquad (42)$$

Clearly, forcing the reaction-diffusion particles and phonons apart has the potential to create instability. This creates the possibility for pattern formation and self organization. The direction of ∇w_D is not necessarily the same as the direction of the concentration gradient producing the diffusion. Indeed the two gradients could point in perpendicular directions. In this diffusion case the results are similar to the electron-phonon case discussed previously [1]. The phonon force leads to a heat transfer equation that is a modified version of the Guyer-Krumhansl equation [15,16,25,26]. The modifications

are shown to lead to instability and possibly spontaneous symmetry breaking if the concentration gradient is strong enough. A simplified version of the partial derivative equation for the temperature field is

$$\frac{c_V}{\kappa}\frac{\partial T}{\partial t} = (1 - \alpha_p)\nabla^2 T + \frac{1}{c_V}\nabla^2 U_d, \qquad (43)$$

where κ is the thermal conductivity, and

$$\alpha_p \equiv \frac{1}{c_V}\frac{\partial w_D}{\partial T}, \qquad (44)$$

is a dimensionless parameter describing the temperature dependence of w_D.

Equation (43) resembles the Swift-Hohenberg equation, which is an important tool for researchers of nonequilibrium systems and has, for example, been successfully utilized to model patterns formed in certain types of Poiseuille flow, laminar flame fronts, trapped ion modes in plasmas, and systems with Eckhaus instabilities such as Rayleigh-Bénard convection [3,27–32]. The most important feature of the Swift-Hohenberg equation is a tunable parameter r which can produce a negative relaxation rate, and instability, at $r = 1$ in

$$\frac{\partial \phi}{\partial t} = (r - 1)\phi - 2\nabla^2\phi$$
$$- \nabla^4\phi - \phi^3 \quad \text{(Swift-Hohenberg equation)}. \qquad (45)$$

In Eq. (43) the first term on the right-hand side is the vital component that gives instability when α_p reaches unity. The distinction is that Eq. (43) is derived from first principles whereas the Swift-Hohenberg equation is a model.

G. Kinematics and energetics

In a system with $\boldsymbol{f}_{\text{rdp}} = 0$, the energetics are quite simple. If a steady state is established by an external agent providing a concentration gradient, with a number current density $\boldsymbol{J}$ and velocity $\boldsymbol{\eta}_0 = \boldsymbol{J}/n_{\text{rdp}}$, which are assumed to point in the $\hat{\boldsymbol{z}}$ direction, then the kinetic energy density is $\kappa_0 = \rho\eta_0^2/2$, where $\rho = \rho_{\text{rdp}}$ is the mass density. If the external agent is disengaged, then η will decrease while the system approaches equilibrium, and all of this initial kinetic energy will be converted into heat by reaction-diffusion particle-phonon scattering. When, however, a spatial gradient exists in $\tau^*\dot{u}_D$, then $\boldsymbol{f}_{\text{rdp}}$ is not zero and some of the initial kinetic energy will not go to the phonon bath, but instead could become mechanical kinetic energy via $\boldsymbol{f}_{\text{rdp}}$. The reaction-diffusion particles can even be pushed by $\boldsymbol{f}_{\text{rdp}}$ in a direction perpendicular to $\boldsymbol{J}$.

Toward integrating Eq. (37) and obtaining kinematics, the gradient in Eq. (37) is characterized by an inverse length parameter α such that $|\nabla(\tau^*\dot{u})| = \alpha\tau^*\dot{u}$. The gradient is assumed to be uniform, pointing in the $\hat{\boldsymbol{x}}$ direction. This leaves Eq. (37) as $\dot{p} = \rho\dot{v} = \frac{1}{3}\alpha\tau^*\dot{u}$, meaning that if τ^* is constant in time, then $\rho v - \frac{1}{3}\alpha\tau^* u$ is a conserved quantity. This result holds even if τ^* changes slowly, as long as τ^* is replaced by $\frac{1}{2}[\tau^*(t) + \tau^*(0)]$. In general, one replaces τ^* with $\langle\tau^*\dot{u}\rangle/\langle\dot{u}\rangle$ where $\langle\ \rangle$ represents time averaging over $[0, t]$, to maintain $\rho v - \frac{1}{3}\alpha\tau^* u$ is a conserved quantity.

The positive definite energy density $u = \int_0^t \dot{u}\,dt$ represents the energy dissipated into the phonon heat bath over the time

period $[0, t]$. The energy $\rho\eta^2/2$ becomes zero when the system returns to equilibrium. If in the final state $\eta \simeq 0$, and u_{tot} is the total amount of energy dissipated into heat by reaction-diffusion particle-phonon scattering, then

$$\Delta v \equiv v_f - v_0 = \frac{\alpha\tau^* u_{\text{tot}}}{3\rho} \qquad (46)$$

is the reaction-diffusion particle velocity boost delivered over the entire approach to equilibrium. If the gradient is indeed uniform then the entire reaction-diffusion particle system will be boosted by a velocity Δv in the direction of the gradient of $\tau^*\dot{u}$. If $v_0 = 0$, then the developed kinetic energy $\frac{1}{2}\rho v_f^2$ represents a remarkable transformation of energy, as otherwise it was to be simply dissipated into heat.

What began as a purely dissipative process is no longer so because of the introduction of a spatial gradient. The terminology becomes challenging; a dissipative process can lead to conversion of mechanical energy into something besides heat. In this case it is kinetic energy though this could subsequently be converted into forms of potential energy such as electrostatic, chemical, etc. The process in general involves dissipation (into heat) as well as conversion. The term *dissipation with conversion* may be apt but the term *exergonic* also works well, a term used frequently in the biochemistry literature [5] and infrequently in the physical sciences literature. Exergonic is similar to exothermic but includes the possibility of the same type of energy conversion discussed here.

When $v_0 = 0$, the exergonic conversion factor is defined in general as

$$e_{\text{ex}} \equiv \frac{\frac{1}{2}\rho v_f^2}{n_{\text{rdp}}E_0}. \qquad (47)$$

where E_0 is the per particle initial energy that is to be dissipated. In this discussion $\kappa_0 = n_{\text{rdp}}E_0$. The dimensionless e_{ex} represents the fraction of the available energy κ_0 that is converted to reaction-diffusion particle kinetic energy. Clearly e_{ex} cannot exceed unity.

In physical scattering processes one expects to see nonequilibrium systems approach equilibrium by dissipating energy exothermically over a period of time into the heat bath. What is described here is different and resembles a type of exergonic process called secondary active transport [5]. This type of transport occurs at biological semipermeable membranes and often involves energetically downhill transport of one type of ion across the membrane coupling to, and resulting in, the energetically uphill transport of another ion across the same membrane. One type of ionic membrane potential is exergonically converted into another. The second law of thermodynamics is not broken because there is no conversion of heat into mechanical or electrical energy. Indeed the whole issue is bypassed. This comparison only goes so far; Here there is no membrane and only one type of reaction-diffusion particle. Below in Sec. III B, the case of two types of diffusing particles is treated and this discussion is resumed.

An expression for energy conservation may be obtained, though not before considering the phonon force, $\boldsymbol{f}_p$. An equal and opposite momentum, $-\rho v_f$ is gained by the phonons. Multiplying by c gives an energy $e_p\kappa_0$, where e_p represents the fraction of the available energy κ_0 that is delivered to the

phonon field specifically by the force f_p. In total the force pair syphons out a fraction $e_{ex} + e_p$ of the available energy κ_0. The expression for energy conservation is

$$\kappa_0 = \tfrac{1}{2}\rho v_f^2 + \rho c v_f + u_{\text{tot}}. \tag{48}$$

Making use of Eq. (46) results in a quadratic equation for v_f with solution

$$v_f = \frac{c}{s}[-1 + \sqrt{1 + s^2 \zeta^2}], \tag{49}$$

where

$$s \equiv \frac{c\alpha\tau^*}{3 + c\alpha\tau^*} \tag{50}$$

is a dimensionless parameter describing the magnitude of the gradient of $\tau^* \dot{u}$, and

$$\zeta \equiv \sqrt{\frac{2 n_{\text{rdp}} E_0}{\rho_{\text{rdp}} c^2}} \tag{51}$$

is another dimensionless parameter describing how far from equilibrium the system is. Furthermore,

$$e_{ex} = s^{-2}\zeta^{-2}[-1 + \sqrt{1 + s^2 \zeta^2}]^2, \tag{52}$$

which can be inverted to

$$\zeta = \frac{2\sqrt{e_{ex}}}{s(1 - e_{ex})}. \tag{53}$$

For the phonons,

$$e_p = 2s^{-1}\zeta^{-2}[-1 + \sqrt{1 + s^2 \zeta^2}]. \tag{54}$$

Equations (52) and (54) were used to make plots of e_{ex} and $e_{ex} + e_p$ versus ζ for two different values of s, as indicated in Fig. 2. The thin solid (blue) curve shows e_{ex} with $\frac{1}{3}c\alpha\tau^* = 0.05$, i.e., under shallow gradient conditions. For $\zeta < 1$, this exergonic conversion coefficient is small but becomes quite significant for $\zeta > 10$, and equals 0.33 at $\zeta = 36.4$. For larger ζ values, Eq. (52) predicts even larger coefficients, eventually approaching unity. The thin short-dash (red) curve shows $e_{ex} + e_p$ which sits very close to the e_{ex} curve at high ζ. For $\zeta \lesssim 10$, e_p exceeds e_{ex} and while $e_{ex} \rightarrow 0$ as $\zeta \rightarrow 0$, e_p instead approaches s. Even near equilibrium, close to 5% of the energy is converted to phonons directed in the opposite direction to the reaction-diffusion particles. This phonon flux could simply result in heat flow. Even so, this differs from typical dissipation which creates heat that flows away from the source equally in all possible directions. It is also possible that the directed phonons represent coherent sound waves. If so, then this energy is not dissipated and could be recovered as useful work. Yet another possibility is that the phonon flux represents second sound waves, also not directly dissipated [7,15]. In cases where the phonon fraction e_p is not dissipated, then $e_{ex} + e_p$ represents the fraction of the available energy that is exergonically converted.

For larger gradients α, the factor e_p becomes more significant. With $\frac{1}{3}c\alpha\tau^* = 0.9$ (steep gradient) the thick solid (black) curve shows that e_{ex} rises monotonically much sooner than the shallow gradient curve, reaching 0.33 at $\zeta = 3.66$. The effect on e_p is even greater; With $\zeta < 1$, e_p is substantially larger than e_{ex}, and as $\zeta \rightarrow 0$, e_p approaches $s = 0.47$. In this
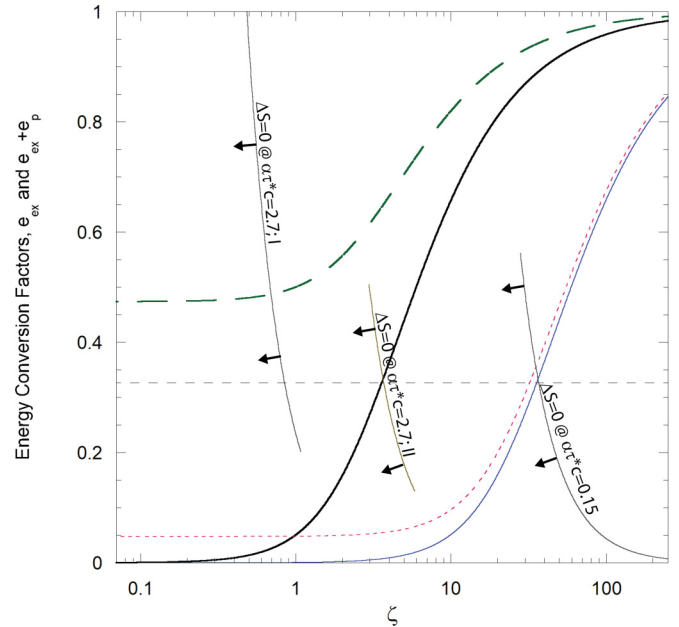

FIG. 2. Energy conversion factors as a function of parameter ζ, characterizing nonequilibrium. With a small gradient value of $\alpha\tau^* c = 0.15$, the thin solid (blue) curve shows the exergonic conversion coefficient, e_{ex} and the thin short-dash (red) curve shows $e_{ex} + e_p$. With a strong gradient value of $\alpha\tau^* c = 2.7$, the thick solid (black) curve shows the exergonic conversion coefficient, e_{ex} and the thick long-dash (green) curve shows $e_{ex} + e_p$.

case almost half of the available energy would be converted either to mechanical reaction-diffusion particle energy or to directional phononic energy.

1. Second law considerations

The second law of thermodynamics can be violated if $\frac{1}{3}c\alpha\tau^*$ exceeds unity. From the force $\frac{1}{3}\alpha\tau^*\dot{u}$ on the phonon field, the power is $\frac{1}{3}c|\alpha|\tau^*\dot{u}$ which is directly compared to $\dot{u}$, the rate at which heat is produced. Accounting also for the power delivered to the reaction-diffusion particles, if the phonon power $\frac{1}{3}c|\alpha|\tau^*\dot{u}$ is also recoverable as useful work, then the rate of entropy production σ_I is given by

$$T\sigma_I = \dot{u} - \tfrac{1}{3}v_f\alpha\tau^*\dot{u} - \tfrac{1}{3}c|\alpha|\tau^*\dot{u}. \tag{55}$$

The $-\frac{1}{3}v_f\alpha\tau^*\dot{u}$ and $-\frac{1}{3}c|\alpha|\tau^*\dot{u}$ terms in Eq. (55) are both antidissipative and will reduce entropy. As discussed above in Sec. II F, the same phonon force f_p produces the $-\frac{1}{3}c|\alpha|\tau^*\dot{u}$ term as well as the pattern-forming $\alpha_p \nabla^2 T$ term in Eq. (43).

By the second law, the net entropy production cannot be negative. This means $s \leqslant 0.5$, and if so, the condition $\sigma_I = 0$ holds if

$$(e_{ex} + e_p)|_{\sigma_I = 0} = \frac{1 - 2s}{s^2 \zeta^2}. \tag{56}$$

For the case of $\frac{1}{3}c\alpha\tau^* = 0.9$, this condition is displayed in Fig. 2 (thin gray solid curve that is the furthest left of the three arrow-labelled curves). The arrows attached to this second law barrier point to the area that is allowed by the second law, where $\sigma_I \geqslant 0$. The second law limits the $e_{ex} + e_p$ curve to a

maximal value of 0.487 attained at $\zeta = 0.693$. At this maximal point 46.1% of the available energy is converted to the phonon flow, with only 2.6% going to the reaction-diffusion particles.

Alternatively, if the phonon power $\frac{1}{3}c|\alpha|\tau^*\dot{u}$ is not recoverable as useful work, and simply becomes more heat, then the rate of entropy production σ_I in Eq. (55) is altered by one minus sign to become:

$$T\sigma_{II} = \dot{u} - \frac{1}{3}v_f\alpha\tau^*\dot{u} + \frac{1}{3}c|\alpha|\tau^*\dot{u}. \tag{57}$$

In this case there is no direct restriction on s and the condition $\sigma_{II} = 0$ holds if

$$e_{ex}|_{\sigma_{II}=0} = \frac{1}{s^2\zeta^2}. \tag{58}$$

Combining this with Eq. (52), one can show that e_{ex} takes the maximal value of $1/3$ at $\zeta_{max} = \sqrt{3}/s$. This is verified for the case of $\frac{1}{3}c\alpha\tau^* = 0.9$, where condition Eq. (58) is displayed in Fig. 2 (thin gray solid curve that is in the middle of the three arrow-labeled curves). The maximal $1/3$ value for e_{ex} is also verified for the case $\frac{1}{3}c\alpha\tau^* = 0.05$ at $\zeta_{max} = 36.4$. In this case of small gradients, the two curves defined by Eq. (56) and Eq. (58) lie on top of each other, thus setting the second law barrier as shown (thin gray solid curve that is the furthest right of the three arrow-labelled curves).

2. Cutoff for τ^* timescale

From Eqs. (11) and (40),

$$w_D = -\frac{1}{3}\bar{\varepsilon}\, n_{rdp}\frac{\tau^*}{\tau_{rdp}}. \tag{59}$$

In this form the magnitude of w_D/n_{rdp} is simply related to the phonon energy scale through the dimensionless ratio of two relevant timescales. The quantity w_D/n_{rdp} is the per particle potential energy. In the cases where τ^* is much smaller than τ_{rdp}, w_D/n_{rdp} is much smaller than $\bar{\varepsilon}$. However, when τ^* greatly exceeds τ_{rdp} the result that w_D/n_{rdp} exceeds $\bar{\varepsilon}$ is unphysical, given that $\bar{\varepsilon}$ is all the energy that is available. If the reaction-diffusion particle collides again before the virtual phonon decays, then τ^* should be cut off by replacing it with τ_{rdp}. The result then is to replace τ^*/τ_{rdp} with $\tau^*/(\tau_{rdp} + \tau^*)$. Introducing $\tilde{\tau} \equiv \tau_{rdp}\tau^*/(\tau_{rdp} + \tau^*)$, Eq. (59) is revised to

$$\frac{w_D}{n_{rdp}} = -\frac{\tilde{\tau}\,\bar{\varepsilon}}{3\tau_{rdp}}. \quad \text{(with cutoff).} \tag{60}$$

This procedure amounts to adding in another exponential factor $\exp(-t'/\tau_{rdp})$ into the second-order collision integrals, such as on the right-hand side of Eq. (4). This factor describes the probability of the reaction-diffusion particle surviving before another phonon collision.

H. Diffusion with several reaction-diffusion particles

The aim is to next develop this theory for the case of reactions, and then combine the results for both reaction and diffusion. Before this, results for diffusion in systems with n distinct reaction-diffusion particles are presented. Each type of reaction-diffusion particle, i, will have a distribution

$g_i(\mathbf{k}_i) \equiv g_i$, $g_i(\mathbf{k}'_i) \equiv g'_i$, and an intrinsic transition probability $\mathcal{W}_{i,\mathbf{k}_i}^{\mathbf{k}'_i,\mathbf{q}''}$. Also

$$\dot{u}_{D,i} = \iiint \varepsilon_{\mathbf{q}''}\{g_i(1 + h_{\mathbf{q}''}) - g'_i h_{\mathbf{q}''}\}\mathcal{W}_{i,\mathbf{k}_i}^{\mathbf{k}'_i,\mathbf{q}''}$$
$$\times \delta(\mathbf{k}_i - \mathbf{k}'_i - \mathbf{q}'')d\mathbf{k}_i d\mathbf{k}'_i d\mathbf{q}'', \tag{61}$$

$$w_{D,i} = -\frac{1}{6}\iiint \tau_> \varepsilon_{\mathbf{q}''}\{g_i(1 + h_{\mathbf{q}''}) - g'_i h_{\mathbf{q}''}\}\mathcal{W}_{i,\mathbf{k}_i}^{\mathbf{k}'_i,\mathbf{q}''}$$
$$\times \delta(\mathbf{k}_i - \mathbf{k}'_i - \mathbf{q}'')d\mathbf{k}_i d\mathbf{k}'_i d\mathbf{q}'', \tag{62}$$

$$\tau_i^* = -3\frac{w_{D,i}}{\dot{u}_{D,i}}. \tag{63}$$

For each type of reaction-diffusion particle,

$$\mathbf{f}_{rdp,D,i} = -\nabla w_{D,i}, \tag{64}$$

while the net force on all the reaction-diffusion particles is

$$\mathbf{f}_{rdp,D} = -\sum_{i=1}^{n}\nabla w_{D,i}. \tag{65}$$

The force pair $\mathbf{f}_{rdp,D}$ and $\mathbf{f}_{p,D}$ still sum up to zero. In the following section on the combination reaction with $n = 3$, the index i will be A, B, or C.

Collisions between different particles is not included yet. This matter will be discussed below in Sec. III B.

III. CASE OF REACTIONS

The approach taken above for diffusion of reaction-diffusion particles via phonon scattering will be applied in similar ways to chemical (and possibly nuclear) reactions. A second-order Boltzmann transport equation is developed combining previously established transport theories for chemical reactions [8–12] and the phonon Boltzmann transport equation [6,17]. The reaction first considered below is the exothermic combination reaction $A + B \rightleftharpoons C$.

Before discussing the second-order scattering, some first-order results are presented. The forward reaction rate for this combination is

$$R_f = \iiiint g_A g_B(1 + h_{\mathbf{q}''})\mathcal{R}_{A,B}^{C,\mathbf{q}''}$$
$$\times \delta(\mathbf{k}_A + \mathbf{k}_B - \mathbf{k}_C - \mathbf{q}'')d\mathbf{k}_A d\mathbf{k}_B d\mathbf{k}_C d\mathbf{q}''. \tag{66}$$

The reverse reaction rate is

$$R_r = \iiiint g_C h_{\mathbf{q}''}\mathcal{R}_{A,B}^{C,\mathbf{q}''}$$
$$\times \delta(\mathbf{k}_A + \mathbf{k}_B - \mathbf{k}_C - \mathbf{q}'')d\mathbf{k}_A d\mathbf{k}_B d\mathbf{k}_C d\mathbf{q}''. \tag{67}$$

The reaction velocity is $v = R_f - R_r$. The rate at which energy is transferred to the phonon field by reactions is

$$\dot{u}_R = \iiiint \varepsilon_{q''} \{g_A g_B (1 + h_{q''}) - g_C h_{q''}\} \mathcal{R}_{A,B}^{C,q''} \delta(\boldsymbol{k}_A + \boldsymbol{k}_B - \boldsymbol{k}_C - \boldsymbol{q}'') d\boldsymbol{k}_A d\boldsymbol{k}_B d\boldsymbol{k}_C d\boldsymbol{q}''. \tag{68}$$

Also,

$$\tau_R^* \equiv \frac{\iiiint \tau_> g_A g_B (1 + h_{q''}) \mathcal{R}_{A,B}^{C,q''} \delta(\boldsymbol{k}_A + \boldsymbol{k}_B - \boldsymbol{k}_C - \boldsymbol{q}'') \varepsilon_{q''} d\boldsymbol{k}_A d\boldsymbol{k}_B d\boldsymbol{k}_C d\boldsymbol{q}''}{\iiiint g_A g_B (1 + h_{q''}) \mathcal{R}_{A,B,q}^{C,q''} \delta(\boldsymbol{k}_A + \boldsymbol{k}_B - \boldsymbol{k}_C - \boldsymbol{q}'') \varepsilon_{q''} d\boldsymbol{k}_A d\boldsymbol{k}_B d\boldsymbol{k}_C d\boldsymbol{q}''}. \tag{69}$$

This form for τ_R^* resembles that of τ^* from Eq. (39) for diffusion. The same arguments as made in Sec. II E apply here and τ_R^* is expected to follow the τ^* rule, just as in the case of diffusion.

A. Second-order scattering processes: Reaction, diffusion, and phonon collisions for the combination reaction

The important collision integral for reactant, A, for the combination reaction

$$A + B \rightleftharpoons C + p,$$
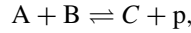
which is exothermic with phonon emission q'', that subsequently scatters as part of a three-phonon scattering process, is

$$\frac{\partial g_A}{\partial t}\bigg|_{R2} = \frac{1}{2} \int_0^\infty \iiiint \Big[\{-e^{-t'/\tau_{1,>}} g_A g_B h_q (1 + h_{q'}) + e^{-t'/\tau_{1,<}} g_C (1 + h_q) h_{q'}\} \mathcal{Q}_{q'',q}^{q'} \delta(\boldsymbol{q}'' + \boldsymbol{q} - \boldsymbol{q}')$$
$$+ \{-e^{-t'/\tau_{2,>}} g_A g_B (1 + h_q)(1 + h_{q'}) + e^{-t'/\tau_{2,<}} g_C h_q h_{q'}\} \mathcal{Q}_{q''}^{q,q'} \delta(\boldsymbol{q}'' - \boldsymbol{q} - \boldsymbol{q}') \Big]$$
$$\times (1 + h_{q''}) h_{q''} \mathcal{R}_{A,B}^{C,q''} \delta(\boldsymbol{k}_A + \boldsymbol{k}_B - \boldsymbol{k}_C - \boldsymbol{q}'') d\boldsymbol{k}_B d\boldsymbol{k}_C d\boldsymbol{q} d\boldsymbol{q}' d\boldsymbol{q}'' dt', \tag{70}$$

where $g_A \equiv g_A(\boldsymbol{k}_A)$ is the electronic distribution function for reactant type A with wave vector $\boldsymbol{k}_A$. Equation (70), along with Eq. (4) for the diffusion case, constitute the reaction-diffusion-phonon Boltzmann transport equation. Making use of Eqs. (14) and (16) and focusing on the forward reaction, well away from equilibrium:

$$\frac{\partial g_A}{\partial t}\bigg|_{R2} = -\int_0^\infty \iiint \Big[e^{-t'/\tau_{1,>}} g_A g_B h_q (1 + h_{q''}) \frac{1}{\tau_{1,>}'} + e^{-t'/\tau_{2,>}} g_A g_B (1 + h_{q''}) \frac{1}{\tau_{2,>}'} \Big] \mathcal{R}_{A,B}^{C,q''} \delta(\boldsymbol{k}_A + \boldsymbol{k}_B - \boldsymbol{k}_C - \boldsymbol{q}'') d\boldsymbol{k}_B d\boldsymbol{k}_C d\boldsymbol{q}'' dt'. \tag{71}$$

The analysis presented here is similar to the first-order theory which results in Enskog's equation of change. The force on reactant, A, is

$$\boldsymbol{f}_A = -\hbar \int_0^\infty \iiiint \boldsymbol{k}_A \Big[e^{-t'/\tau_{1,>}} g_A g_B (1 + h_{q''}) \frac{1}{\tau_{1,>}'} + e^{-t'/\tau_{2,>}} g_A g_B (1 + h_{q''}) \frac{1}{\tau_{2,>}'} \Big] \mathcal{R}_{A,B}^{C,q''}$$
$$\times \delta(\boldsymbol{k}_A + \boldsymbol{k}_B - \boldsymbol{k}_C - \boldsymbol{q}'') d\boldsymbol{k}_A d\boldsymbol{k}_B d\boldsymbol{k}_C d\boldsymbol{q}'' dt'. \tag{72}$$

Similarly,

$$\frac{\partial g_B}{\partial t}\bigg|_{R2} = -\int_0^\infty \iiint \Big[e^{-t'/\tau_{1,>}} g_A g_B h_q (1 + h_{q''}) \frac{1}{\tau_{1,>}'} + e^{-t'/\tau_{2,>}} g_A g_B (1 + h_{q''}) \frac{1}{\tau_{2,>}'} \Big] \mathcal{R}_{A,B}^{C,q''}$$
$$\times \delta(\boldsymbol{k}_A + \boldsymbol{k}_B - \boldsymbol{k}_C - \boldsymbol{q}'') d\boldsymbol{k}_A d\boldsymbol{k}_C d\boldsymbol{q}'' dt', \tag{73}$$

$$\boldsymbol{f}_B = -\hbar \int_0^\infty \iiiint \boldsymbol{k}_B \Big[e^{-t'/\tau_{1,>}} g_A g_B (1 + h_{q''}) \frac{1}{\tau_{1,>}'} + e^{-t'/\tau_{2,>}} g_A g_B (1 + h_{q''}) \frac{1}{\tau_{2,>}'} \Big] \mathcal{R}_{A,B}^{C,q''}$$
$$\times \delta(\boldsymbol{k}_A + \boldsymbol{k}_B - \boldsymbol{k}_C - \boldsymbol{q}'') d\boldsymbol{k}_A d\boldsymbol{k}_B d\boldsymbol{k}_C d\boldsymbol{q}'' dt', \tag{74}$$

and

$$\frac{\partial g_C}{\partial t}\bigg|_{R2} = \int_0^\infty \iiint \Big[e^{-t'/\tau_{1,>}} g_A g_B h_q (1 + h_{q''}) \frac{1}{\tau_{1,>}'} + e^{-t'/\tau_{2,>}} g_A g_B (1 + h_{q''}) \frac{1}{\tau_{2,>}'} \Big] \mathcal{R}_{A,B}^{C,q''}$$
$$\times \delta(\boldsymbol{k}_A + \boldsymbol{k}_B - \boldsymbol{k}_C - \boldsymbol{q}'') d\boldsymbol{k}_A d\boldsymbol{k}_B d\boldsymbol{q}'' dt', \tag{75}$$

$$\boldsymbol{f}_C = \hbar \int_0^\infty \iiiint \boldsymbol{k}_C \Big[e^{-t'/\tau_{1,>}} g_A g_B (1 + h_{q''}) \frac{1}{\tau_{1,>}'} + e^{-t'/\tau_{2,>}} g_A g_B (1 + h_{q''}) \frac{1}{\tau_{2,>}'} \Big] \mathcal{R}_{A,B}^{C,q''}$$
$$\times \delta(\boldsymbol{k}_A + \boldsymbol{k}_B - \boldsymbol{k}_C - \boldsymbol{q}'') d\boldsymbol{k}_A d\boldsymbol{k}_B d\boldsymbol{k}_C d\boldsymbol{q}'' dt'. \tag{76}$$

By conservation of momentum, $\boldsymbol{k}_A + \boldsymbol{k}_B - \boldsymbol{k}_C = \boldsymbol{q}''$. Thus, adding Eqs. (72), (74), and (76):

$$\boldsymbol{f}_A + \boldsymbol{f}_B + \boldsymbol{f}_C = -\hbar \int_0^\infty \iiiint \boldsymbol{q}'' \left[e^{-t'/\tau_{1,>}} g_A g_B (1 + h_{\boldsymbol{q}''}) \frac{1}{\tau'_{1,>}} + e^{-t'/\tau_{2,>}} g_A g_B (1 + h_{\boldsymbol{q}''}) \frac{1}{\tau'_{2,>}} \right] \mathcal{R}_{A,B}^{C,\boldsymbol{q}''}$$
$$\times \delta(\boldsymbol{k}_A + \boldsymbol{k}_B - \boldsymbol{k}_C - \boldsymbol{q}'') d\boldsymbol{k}_A d\boldsymbol{k}_B d\boldsymbol{k}_C d\boldsymbol{q}'' dt', \tag{77}$$

The net force on the reactant-diffusion particles includes both reactants and products: $\boldsymbol{f}_{\mathrm{rdp},R} \equiv \boldsymbol{f}_A + \boldsymbol{f}_B + \boldsymbol{f}_C$. The analysis for the phonon force is similar to that for diffusion in Sec. II and is carried out in Appendix B. Comparing to Eq. (B7), one verifies the expected momentum-conserving result:

$$\boldsymbol{f}_{p,R} = -\boldsymbol{f}_{\mathrm{rdp},R}. \tag{78}$$

Thus, in both cases considered so far, the phonon force is equal and opposite to the net force on all the other particles. Note that it is not strictly a force pair in this case. It is a quartet (multiplet in general) of forces that are constrained in the way described by Eq. (78). Nevertheless, the term force pair will continue to be employed for $\boldsymbol{f}_{\mathrm{rdp},R}$ and $\boldsymbol{f}_{p,R}$.

These results are quite general and there are many important examples of combinations reactions involving atoms and/or small molecules: Ex. $\mathrm{Fe} + \mathrm{S} \rightarrow \mathrm{FeS}$. Larger molecules and clusters are included as well. Indeed, if B is a large cluster then the reaction very much resembles adsorption of A onto a substrate B. Both physisorption and chemisorption are covered by this analysis and the example of such adsorption processes onto tiny dust grains is also covered by this theory. For example, the processes by which the interstellar medium evolves toward star formation would be covered, and partly governed, by Eq. (78). Nuclear combination reactions are also covered by this formalism. Examples include the absorption of an α particle by a larger nucleus and the fusion of two nuclei in general.

The spatial variation is treated very similarly to the diffusion case:

$$g_A g_B (1 + h_{\boldsymbol{q}''}) \mathcal{R}_{A,B}^{C,\boldsymbol{q}''} \big|_{\boldsymbol{r} - \Delta \boldsymbol{r}} = g_A g_B (1 + h_{\boldsymbol{q}''}) \mathcal{R}_{A,B}^{C,\boldsymbol{q}''} \big|_{\boldsymbol{r}}$$
$$- \Delta \boldsymbol{r} \cdot \nabla \left\{ g_A g_B (1 + h_{\boldsymbol{q}''}) \mathcal{R}_{A,B}^{C,\boldsymbol{q}''} \right\}. \tag{79}$$

The same issues exist as with diffusion, with a nonzero force when in equilibrium. From here on it is assumed the reaction is proceeding strongly in the forward (exothermic) direction such that

$$\dot{u}_R = \iiiint g_A g_B (1 + h_{\boldsymbol{q}''}) \mathcal{R}_{A,B}^{C,\boldsymbol{q}''}$$
$$\times \delta(\boldsymbol{k}_A + \boldsymbol{k}_B - \boldsymbol{k}_C - \boldsymbol{q}'') \varepsilon_{\boldsymbol{q}''} d\boldsymbol{k}_A d\boldsymbol{k}_B d\boldsymbol{k}_C d\boldsymbol{q}''. \tag{80}$$

The net force on all reactant-diffusion particles is

$$\boldsymbol{f}_{\mathrm{rdp},R} = -\nabla w_R, \tag{81}$$

where

$$w_R = -\tfrac{1}{3} \tau_R^* \dot{u}_R. \tag{82}$$

In this section it has so far been assumed that the reactants A and B are distinguishable. If they are not, such as in the oxygen combination reaction $\mathrm{O} + \mathrm{O} \rightarrow \mathrm{O}_2$, then there is an over counting problem with integrating $d\boldsymbol{k}_A d\boldsymbol{k}_B$, and in all of the integrals in Eqs. (66), (67), (69), (72), (74), (76), (77), (80), and (83), a factor of $\frac{1}{2}$ should be inserted as a correction. The important results in Eqs. (81) and (82) remain the same.

Another issue concerns internal modes of molecules. The summations over variables such as $\boldsymbol{k}_A$ can easily be adapted to include a sum over quantum numbers describing the internal modes of particle A. This would include rotational quantum numbers. In any integral, $d\boldsymbol{k}_A$ will be understood to include these sums. The transition probability $\mathcal{R}_{A,B}^{C,\boldsymbol{q}''}$ will depend on these quantum numbers and make the force calculations more complicated. The same added complications are present in Eq. (80) for $\dot{u}_R$, leaving Eq. (82) unaltered.

1. Near equilibrium expansion

In Appendix C, near equilibrium expansions are calculated for the case of concentration gradients in A, B, and C, as well as the case of nonzero chemical affinity. Any combination of these effects will result in a nonzero $\dot{u}_R$ and w_R. A concentration gradient in any of A, B, C, will contribute to $\dot{u}_R$ by reaction as well as direct diffusion, as discussed in Sec. II. Combining all the relevant near equilibrium processes, gives explicitly

$$\dot{u}_R = \iiiint \left[\frac{2}{3} \beta^2 \left(\sum_i K_i \right) \varepsilon_{\boldsymbol{q}''} + \beta A \right] g_A^0 g_B^0 (1 + h_{\boldsymbol{q}''}^0) \mathcal{R}_{A,B}^{C,\boldsymbol{q}''}$$
$$\times \delta(\boldsymbol{k}_A + \boldsymbol{k}_B - \boldsymbol{k}_C - \boldsymbol{q}'') \varepsilon_{\boldsymbol{q}''} d\boldsymbol{k}_A d\boldsymbol{k}_B d\boldsymbol{k}_C d\boldsymbol{q}'', \tag{83}$$

where $\sum_i K_i = K_A + K_B + K_C$. In the $\sum_i K_i$ contributions, either concentration gradients drive reaction or reaction attenuates concentration gradients.

2. Effect of reactions on the phonon field

As in the case of diffusion, the force $\boldsymbol{f}_{p,R}$ is equal and opposite to $\boldsymbol{f}_{\mathrm{rdp},R}$, and will also modify the equations for heat flow. Instabilities are possible if α_p from Eq. (43) is large enough. An unstable Eq. (43) can lead to pattern formation in the temperature profile and this would certainly affect the reaction-diffusion particles and create similar patterns in the reaction-diffusion particle density. Spontaneous symmetry breaking is possible. This can happen in a system initially free of any concentration and temperature gradients, if the affinity is simply raised to a threshold value. This possibility does not exist for pure diffusion, but does exist in reactive systems.

When thermal gradients do exist, $\boldsymbol{f}_p$ could, in principle, direct phonons toward regions of higher temperature, i.e., against the direction of conventional heat flow as described by Fourier's law. In this case one can say that $\boldsymbol{f}_p$ actively transports phonons, and the active transport concept is extended to quasiparticles.

A similar result was claimed in Ref. [33], i.e., when the affinity in a reaction-diffusion system reaches a threshold,
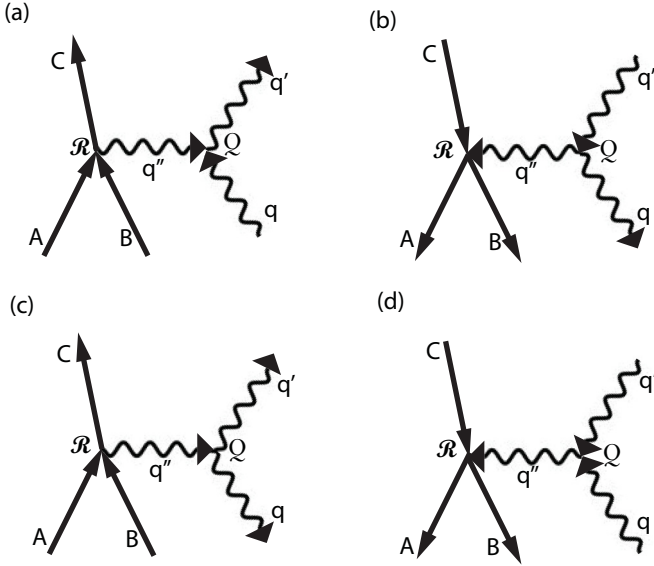
FIG. 3. Second-order reactant-diffusion particle-phonon scattering diagrams, for the combination reaction, covering all cases with three-phonon scattering. Two vertices are present, labeled $\mathcal{R}$ for reactant-diffusion particle-phonon reaction and $\mathcal{Q}$ for phonon-phonon interaction.

patterns may form after the breaking of spatial symmetry. In Ref. [33] a different approach was taken, one based on general thermodynamics and entropy creation. The approach is lacking in microscopic detail with τ^* being a general fluctuation timescale, whereas here it is more specifically defined. Also, in this work, momentum conservation between reaction-diffusion particles and phonons is clearly stipulated. Here, the influence of entropy creation is not as clear, but the results are similar. From Fig. 3 it is clear that multiple phonons are created when reactions release energy. Phonon number is not conserved and the created phonons become part of the thermal bath. The forward reaction is favored over the reverse because it creates more entropy. By going to the second-order transport integrals, the entropy creation is explicitly clear.

Pattern formation in reaction-diffusion systems was first proposed by Turing as an example of bifurcation in nonlinear dynamical systems [2]. Producing such patterns proved to be difficult, taking almost 40 years. Systems that have shown pattern formation include the well-studied chlorite-iodide-malonic acid (CIMA) reaction and the Belousov-Zhabotinsky (BZ) reaction which involves bromide and bromous acid [34–39]. For example, the CIMA reaction is known for producing two-dimensional patterns possessing clear crystal-like symmetry, some with hexagonal patterns, others resembling modulated stripes, as well as mixed states [3,32,34–36].

The results presented here suggest that heat transfer plays an important role in initiating pattern formation. Of course, the simple reaction treated so far will not completely describe the rather complicated CIMA and BZ reactions and more study is required before concluding that heat transfer via the phonon force $\boldsymbol{f}_{p,R}$ lies at the heart of pattern formation in the CIMA and BZ systems.

3. Relaxation of excited reaction-diffusion particles

Since the combination reaction is inelastic, the product C will likely emerge in an excited state, C*. This includes electronic, rotational, and internal vibronic excitations. The products could also be described as hot. One way these hot particles C* can de-excite is by emission of a phonon, i.e., C* → C*+ p. Multiple phonon emission may be required to bring the reaction-diffusion particle to its ground state C. Each step would be described by the processes shown in Fig. 1.

One may think of the de-excitation as diffusion or equivalently as a simple type of chemical reaction in which the per particle excitation energy E^* plays the role of de Donder's chemical affinity A. Borrowing from the analysis in Appendix C a good approximation for $\dot{u}$ is given by

$$\dot{u}_{\text{exc}} = \beta E^* \iiint g_k^0 \left(1 + h_{q''}^0\right) \mathcal{W}_{\text{exc},k}^{k',q''}$$
$$\times \, \delta(\boldsymbol{k} - \boldsymbol{k}' - \boldsymbol{q}'') \varepsilon_{q''} d\boldsymbol{k} d\boldsymbol{k}' d\boldsymbol{q}''. \tag{84}$$

For this type of relaxation $\bar{\varepsilon}$ is replaced by E^*, which may often be substantially larger. Equation (60) becomes

$$\frac{w_{\text{exc}}}{n_C} = -\frac{\tilde{\tau} \, E^*}{3\tau_{\text{rdp}}}. \tag{85}$$

This type of relaxation can be important because a significant part of the energy dissipated by chemical reaction occurs by excited reaction products. Generally, the excited product C* de-excites by emitting phonons and/or infared photons.

Returning briefly to the energetics discussion of Sec. II G, the initial (and assumed positive) affinity, A_0, acts as E_0, in Eq. (51), for example. In this discussion of excited reaction-diffusion particles, $E_0 = E^*$. Thus, ζ, as well as e_{ex} and e_p, can be calculated for reactions in general, in addition to the case of diffusion.

4. Individual reaction-diffusion particle forces and potentials

The analysis presented here identifies an equal and opposite force pair, $\boldsymbol{f}_{\text{rdp}}$ and $\boldsymbol{f}_p$, though it is really a force quartet, $\boldsymbol{f}_A, \boldsymbol{f}_B, \boldsymbol{f}_C$, and $\boldsymbol{f}_p$, which add up to zero. The force $\boldsymbol{f}_{\text{rdp}}$ is the net force on all the reaction-diffusion particles in question, and any resulting solutions for the motion, based on knowledge of $\boldsymbol{f}_{\text{rdp}}$, would be for the center of mass of the reaction-diffusion particles.

Example calculations made below are based on making good estimates for $\dot{u}$, which in turn allows for good estimates of $\boldsymbol{f}_{\text{rdp}}$. Unfortunately this does not work on the constituents such as A, B, and C. For these forces, one must evaluate the integrals in Eqs. (72), (74), and (76), and a good method for estimating these integrals has not yet been determined.

If A and B were to be similar in internal structure, have similar masses, as well as having the same concentration gradients in a combination reaction, then they would experience approximately the same force vector. This is as far as one can go at this stage. For example, it is possible for the two reaction-diffusion particles, B and C, to have forces pointing in opposite directions.

Even if the various reaction-diffusion particles were to receive different accelerations and impulses, subsequent first-order diffusion will tend to make all velocities equal. For

example, the force f_{rdp} acting on hot product reaction-diffusion particles may be substantial if E^* is large and these products would receive more momentum than both reactants and the not so highly excited products. Diffusion via bimolecular collisions in general (not necessarily producing phonons) is important in slowing down the higher velocity products. One effect of first-order scattering is to create an overall reaction-diffusion particle flow that has a unique local velocity, $\mathbf{v}_{rdp}$. Nevertheless, if for example, f_B and f_C are strong enough and do not point in the same direction then a unique local velocity may not be possible. If so, then each type of reaction-diffusion particle would have its own flow velocity.

5. Primary active transport

Focusing on one particular reactant A, the force f_A can be aligned against the concentration gradient in n_A, thus, in opposition to diffusion. In this case the process is described as pushing particles of type A uphill energetically, in contrast to the downhill motion of diffusion. The best term to describe this uphill force is primary active transport [5]. In primary active transport, energy is released from a chemical reaction with some fraction going toward pushing type A particles uphill. If only type A particles are being pushed uphill, then this fraction is the exergonic conversion factor e_{ex}.

It is known that primary active transport occurs in biological systems. For example, in mitochondria, protons are pumped uphill during glycolysis. The protons are pumped through a thin (7-nm-thick) inner membrane to the inside matrix region where the potential is higher by 50 meV [5]. The pumping of protons is an important first step of Mitchell's general chemiosmotic mechanism [4]. The second step involves having the energy stored in this proton potential being used to promote ADP molecules to the higher energy form of ATP.

If a proton, with mass m_P, is involved in a combination reaction which releases energy E_0, then an amount of energy $e_{ex}E_0$ is available to be converted into kinetic energy of protons, which can then become stored as electrostatic energy right up to the proton potential of 50 meV. Toward calculating s, using Eq. (50), the speed of sound in water of 1482 m/s is used for c, an estimate of 1 ps is taken for τ^*, and the inverse of the membrane thickness gives $\alpha = 1.4 \times 10^8$ m^{-1}. This gives $\alpha c \tau^* = 0.207$, and $s = 0.065$, using Eq. (50). With a value of $E_0 = 8.2$ eV, $\zeta = 26.7$, after using Eq. (51), and the result for the exergonic conversion factor is $e_{ex} = 0.33$.

The estimate for τ^* comes from thermal conductivity data on electrical insulators such as LiF and NaCl. These are used since electrical contributions to the thermal conductivity are negligible. The following expression is used:

$$\kappa = \tfrac{1}{3}c_V c^2 \tau^*, \tag{86}$$

where κ is the lattice specific heat and c_V is the volume specific heat capacity. For NaCl at room temperature, $\tau^* = 0.86$ ps [7]. This value is considered to be a good representative value for liquids and solids; thus, 1 ps is to be utilized when detailed knowledge of τ^* is lacking. For example, for dilute gases, τ^* will be larger. Though it may well be that low density systems will display effects of the force pair very well, the examples presented here are all for liquids and solids.

The results from these simple calculations for e_{ex} are very encouraging. About one-third of the available 8.2 eV will be converted into proton kinetic energy. This energy may then be used to drive other processes such as converting ADP to the higher energy ATP. The energy conversion happens without violating the second law. The numerical estimates used in this calculation lie very close to both of the second law barriers defined by Eqs. (56) and (58). Given that these are just estimates, anything close to $\sigma = 0$ should be considered as a positive result, and there is no clear violation of the second law.

The 8.2 eV energy value is reasonable; One glucose molecule releases about three times E_0. Also, if τ^* were to take a larger, and still plausible, value of 3 ps, then the same e_{ex} is obtained with a lower E_0 value of 1.2 eV. This energy release E_0 is in line with many reactions; for example, it is about twice the energy released by ATP conversion to ADP. Though it is clear that there is complexity in the multistep glycolysis process that has not been explained so far, the discussion presented below makes the case that each reaction step can produce a force pair, and thus entire processes such as the citric acid cycle could be covered, step by step, by this formalism.

Showing that e_{ex} can, with reasonable numbers, be in the range of one-third, is important, but not the whole story. It must also be shown that a proton potential near 50 meV can be built up. This discussion will wait until the example system discussed in Sec. VII.

6. Special case where $n_B \ll n_A$

For the simple combination reaction discussed here, the reaction rate can be limited when one reactant concentration greatly exceeds the other. For example, if $n_B \ll n_A$, then n_B represents a bottleneck. If the masses m_A and m_B are close to equal, then the two force densities f_A and f_B are expected to be near equal. The two per particle forces defined as f_A/n_A, and f_B/n_B, will be very different in magnitude. This can be understood if one focuses on a single reaction and the surrounding volume $1/n_B$. The impulse delivered to A and B particles will, on average, be about the same, but, with most A particles not participating, the impulse averaged over all type A reactants will be much smaller than it is for type B reactants. If the forces f_A and f_B are expressed as $f_A = -\nabla w_A$ and $f_B = -\nabla w_B$, then the per particle potential energy w_B/n_B will be much stronger than w_A/n_A.

A good example of such a chemical bottleneck is when reactant B is a proton. Under typical conditions such as a pH value of 7, the concentration of protons can easily be 7 orders of magnitude lower than for other reactants and products.

This second-order transport type of bottleneck differs from previously reported instances [40–42] and helps to show that the bottleneck or gating effect can arise in many different circumstances.

B. Bimolecular reactions and beyond

This formalism is well suited to also describe bimolecular reactions $A + B \rightleftharpoons C + D + p$. These reactions have been well-studied using the first-order Boltzmann transport/reaction equation [8–12].
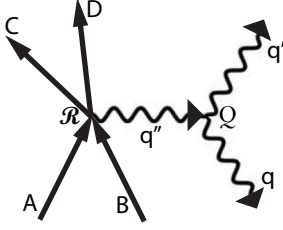
FIG. 4. Second-order reaction-diffusion particle-phonon scattering diagrams, for bimolecular reaction, representative example.

Following the second-order scattering approach of Sec: III (see Fig. 4) yields the following results:

$$
\dot{u}_{bi,R} = \iiiint \varepsilon_{q''}\{g_A g_B(1 + h_{q''}) - g_C g_D h_{q''}\}\mathcal{R}_{A,B}^{C,D,q''}
$$
$$
\times \delta(\boldsymbol{k}_A + \boldsymbol{k}_B - \boldsymbol{k}_C - \boldsymbol{k}_D - \boldsymbol{q}'')d\boldsymbol{k}_A d\boldsymbol{k}_B d\boldsymbol{k}_C d\boldsymbol{k}_D d\boldsymbol{q}'',
$$

(87)

and

$$
w_{bi,R} = -\frac{1}{3}\iiiint \bar{\tau}_> \varepsilon_{q''}\{g_A g_B(1 + h_{q''}) - g_C g_D h_{q''}\}\mathcal{R}_{A,B}^{C,D,q''}
$$
$$
\times \delta(\boldsymbol{k}_A + \boldsymbol{k}_B - \boldsymbol{k}_C - \boldsymbol{k}_D - \boldsymbol{q}'')d\boldsymbol{k}_A d\boldsymbol{k}_B d\boldsymbol{k}_C d\boldsymbol{k}_D d\boldsymbol{q}''.
$$

(88)

The prefactors for these integrals would be adjusted according to whether any participating particles are identical. However, in all cases regarding indistinguishability, the following two relations hold:

$$
w_{\text{bi},R} = -\tfrac{1}{3}\tau_{\text{bi},R}^* \dot{u}_{\text{bi},R}
$$

(89)

and

$$
\boldsymbol{f}_{\text{bi,rdp}} = -\boldsymbol{f}_{\text{bi},p} = -\nabla w_{\text{bi},R}.
$$

(90)

Potential differences are easily calculated since the forces are presented here as gradients. For the reaction-diffusion particles all together the potential energy density is $w_{\text{bi},R}$.

This case also describes a simple collision between two different particles that would occur in a multicomponent diffusing system. For example, if particles A and B differ but A and C are the same, and B and D are also the same, then this type of diffusion is covered. This completes the diffusion possibilities for multicomponent systems.

1. Secondary active transport

Returning to the topic of secondary active transport, if there are two reaction-diffusion particles, A and B, scattering, and if the system is initially set up with a gradient in the concentration n_A of A, with n_B uniform, then there is now a clear force on B particles that will break the symmetry of the concentration profile n_B. The B particles will be pushed

uphill energetically then as the A system moves downhill. A membrane is not necessary to make this coupling work. However, a membrane may facilitate the maintaining of large gradients. This may especially be true if the relevant reaction-diffusion particles are charged. A membrane could withstand large internal electric fields and potential differences ΔV_A and ΔV_B across the membrane could become significant. If an external agent can maintain the gradient in the concentration, n_A, then a significant potential ΔV_B can be held indefinitely. The coupling described here is noteworthy and becomes a good candidate for a physical mechanism for secondary active transport.

In biological systems the two types of particles could be Na^+ ions and Ca^{2+} ions. In a well-studied example, Na^+ ions transport downhill while Ca^{2+} ions are pushed uphill [5]. For the Ca/Na case the two ions move in opposite directions. In other systems one reaction-diffusion particle moves downhill while the other moves uphill in the same direction, for example, protons and lactase [5]. This emphasizes how well suited this second-order transport is for describing these systems; The two physical flow directions, energetically uphill and downhill, are not restricted.

2. Beyond bimolecular reactions

More complicated reactions are described much the same way. For a given system there may be μ_R possible reactions, with channel index μ running from 1 to μ_R. For a given reaction channel μ, there are m_μ reactants and n_μ products, meaning there are $m_\mu + n_\mu + 1$ integrals to perform, including the $\boldsymbol{q}''$ integral.

The intrinsic reaction transition probability, fully labeled, becomes $\mathcal{R}_{\mu,1,\ldots,m_\mu}^{m_\mu+1,\ldots,m_\mu+n_\mu,\boldsymbol{q}''}$. For the combination reaction, $m_\mu = 2$, $n_\mu = 1$, while for a different μ, $m_\mu = 2$, $n_\mu = 2$, for the bimolecular reaction. This formalism can account for both reactions and diffusion. For simple gradient driven diffusion, $m_\mu = 1$, $n_\mu = 1$, while for de-excitation of a single excited reaction-diffusion particle, $m_\mu = 1$, $n_\mu = 1$, with a different set of indices μ. The results are summarized here, again focusing on the forward reaction, where the affinity is positive, and well away from equilibrium. Most of these reactions would be exothermic, but when the number of products exceeds the number of reactants, the reactions may be endothermic with $A > 0$. For the dissipation rate,

$$
\dot{u}_\mu = -\frac{1}{3}\int \ldots \int \varepsilon_{q''} g_1 \ldots g_{m_\mu}(1 + h_{q''})\mathcal{R}_{\mu,1,\ldots,m_\mu}^{m_\mu+1,\ldots,m_\mu+n_\mu,\boldsymbol{q}''}
$$
$$
\times \delta\big(\Sigma_{i=1}^{m_\mu}\boldsymbol{k}_i - \Sigma_{j=m_\mu+1}^{m_\mu+n_\mu}\boldsymbol{k}_j - \boldsymbol{q}''\big)d\boldsymbol{k}_1 \ldots d\boldsymbol{k}_{m_\mu+n_\mu}d\boldsymbol{q}'',
$$

(91)

while for the forces on reactants,

$$
\boldsymbol{f}_{\mu,i} = -\hbar\int \ldots \int \boldsymbol{k}_i \bigg[e^{-t'/\tau_{1,>}} g_1 \ldots g_{m_\mu}(1 + h_{q''})\frac{1}{\tau_{1,>}'} + e^{-t'/\tau_{2,>}} g_1 \ldots g_{m_\mu}(1 + h_{q''})\frac{1}{\tau_{2,>}'} \bigg]\mathcal{R}_{\mu,1,\ldots,m_\mu}^{m_\mu+1,\ldots,m_\mu+n_\mu,\boldsymbol{q}''}
$$
$$
\times \delta\big(\Sigma_{i=1}^{m_\mu}\boldsymbol{k}_i - \Sigma_{j=m_\mu+1}^{m_\mu+n_\mu}\boldsymbol{k}_j - \boldsymbol{q}''\big)d\boldsymbol{k}_1 \ldots d\boldsymbol{k}_{m_\mu+n_\mu}d\boldsymbol{q}''dt',
$$

(92)

with $i = 1, \dots m_\mu$. For products,

$$f_{\mu,i} = \hbar \int \dots \int k_i \left[e^{-t'/\tau_{1,>}} g_1 \dots g_{m_\mu}(1 + h_{q''}) \frac{1}{\tau'_{1,>}} + e^{-t'/\tau_{2,>}} g_1 \dots g_{m_\mu}(1 + h_{q''}) \frac{1}{\tau'_{2,>}} \right] \mathcal{R}^{m_\mu+1,\dots,m_\mu+n_\mu,q''}_{\mu,1,\dots,m_\mu}$$
$$\times \delta\left(\Sigma_{i=1}^{m_\mu} k_i - \Sigma_{j=m_\mu+1}^{m_\mu+n_\mu} k_j - q''\right) dk_1 \dots dk_{m_\mu+n_\mu} dq'' dt', \tag{93}$$

with $i = m_\mu + 1, \dots m_\mu + n_\mu$. The potential energy is

$$w_\mu = -\frac{1}{3} \int \dots \int \tau_> \varepsilon_{q''} g_1 \dots g_{m_\mu}(1 + h_{q''}) \mathcal{R}^{m_\mu+1,\dots,m_\mu+n_\mu,q''}_{\mu,1,\dots,m_\mu} \delta\left(\Sigma_{i=1}^{m_\mu} k_i - \Sigma_{j=m_\mu+1}^{m_\mu+n_\mu} k_j - q''\right) dk_1 \dots dk_{m_\mu+n_\mu} dq'', \tag{94}$$

while

$$\tau_\mu^* = -3 w_\mu / \dot{u}_\mu. \tag{95}$$

The total force on the reaction-diffusion particles is

$$f_{\mu,\text{rdp}} = -f_{\mu,p} = -\nabla w_\mu, \tag{96}$$

where the net reaction-diffusion particle force for reaction μ is summed up over all reactants and products as

$$f_{\mu,\text{rdp}} = \sum_{i=1}^{m_\mu+n_\mu} f_{\mu,i}. \tag{97}$$

Again, the same arguments as made in Sec. II E apply to all possible reactions, and τ_μ^* is expected to follow the τ^* rule, i.e., to a good approximation τ_μ^* is independent of μ.

Summing up over all possible processes, both reaction and diffusion types, gives $w = \Sigma_{\mu=1}^{\mu_R} w_\mu$ and

$$f_{\text{rdp}} = \sum_{\mu=1}^{\mu_R} f_{\mu,\text{rdp}} = -\sum_{\mu=1}^{\mu_R} \nabla(w_\mu) = \frac{1}{3} \sum_{\mu=1}^{\mu_R} \nabla(\tau_\mu^* \dot{u}_\mu) = -f_p. \tag{98}$$

If the τ^* rule holds, then $f_{\text{rdp}} = \frac{1}{3} \nabla(\tau^* \dot{u})$, where $\dot{u} = \Sigma_{\mu=1}^{\mu_R} \dot{u}_\mu$.

An important subcase leads to the important example when one reactant and one product are the same. This covers the case when a catalyst C is present for the reaction. For a catalyzed reaction μ, the catalyst will feel a force $f_{\mu,C}$ which contributes to the total $f_{\mu,\text{rdp}}$.

In summary, the general situation can be described quite simply; Any reaction-diffusion process that creates heat does so at the microscopic level by producing phonons via specific scattering vertices. Application of the Enskog equation of change technique, along with conservation of momentum, always produces the force pair. One member of this pair is the phonon force, and the equal and opposite member is the total force on all involved reaction-diffusion particles. The presence of spatial gradients, as discussed, makes these forces nonzero.

IV. SEPARATION THEOREM

After working out transport integrals for both diffusion and reaction, one is lead to the conclusion that for all reaction-diffusion systems, the net force on all reaction-diffusion particles is equal and opposite to the net force on phonons, as stated in Eq. (98). This result is quite general and shows that in reaction-diffusion systems, reaction-diffusion particles

and phonons will always feel forces pushing them away from each other and leading to separation. This is presented as a theorem:

A. Separation theorem

For reaction-diffusion systems, there exists a net force on the reaction-diffusion particles, f_{rdp}, and a force, f_p, on the phonons such that

$$f_{\text{rdp}} = -f_p, \tag{99}$$

with $f_{\text{rdp}} = -\nabla w$.

These forces would appear to be zero in equilibrium and are certainly small near equilibrium. It is only for systems well away from equilibrium that these forces emerge into significance. Whenever these forces have significance in a reaction-diffusion system, the dynamical equations must account for inertial effects and these equations would resemble the Navier-Stokes equations for fluids. Most importantly, a continuum version of Newton's second law exists for the center of mass of the reaction-diffusion particles. Among other terms contributing to $\rho \dot{v}_{\text{rdp}}$ is f_{rdp}. Phonon dynamics are also affected, as discussed in Sec. II F, with the result of a modified Guyer-Krumhansl equation.

B. Particle baths other than phonons

Clearly $\dot{u}$ accounts only for energy dissipated into the phonon field and that there may some of the initial stored per particle energy E_0 that gets dissipated away into other particle fields other than phonons. These forms include photons of course and could also include more exotic types of quasiparticles such as spin waves.

If spin waves play an important role in a given system, then the analysis would look very similar to what has been presented here for phonons. The separation theorem would look the same except that $\dot{u}$ would now represent the rate at which energy is dissipated into spin waves. The spin waves would build up in the system much like phonons do to create their heat bath and there would indeed be a thermal bath of spin waves. The result would be that one could still write the total force in the separation theorem in terms of $\dot{u}$, if $\dot{u}$ includes both scattering into phonons and scattering into spin waves.

It is notable that the separation theorem concerns phonons and phonon scattering and yet does not make specific reference to the precise details of the phonon dispersion relation. For example, for the case of the adsorption reaction for a system with a solid-liquid interface, there is one phonon dis-

persion relation for the liquid phase, and another for the solid phase which may be directional for a solid crystal. There will also be phonons specific to the interface and propagating only along the interface. Yet the expression $f_{\text{rdp}} = \frac{1}{3}\nabla(\tau^*\dot{u})$ remains the same. The same argument holds for the spin waves and any other relevant quasiparticles. As long as one knows the spatial distribution of how energy is dissipated then the forces in the separation theorem can be calculated.

For the case of a system with both phonons and spin waves, Eq. (99) would be modified to

$$f_{\text{rdp}} = -f_p - f_{\text{spin}}, \tag{100}$$

with $f_{\text{spin}} = \nabla w_{\text{spin}}$. Note that for the two examples, phonons and spin waves, discussed so far, both are examples of Goldstone bosons, created as a result of spontaneous symmetry breaking. After symmetry is broken, a nonzero order parameter is created and the Goldstone bosons describe the oscillating, gapless, wave modes of this order. Thus, any force that acts on the Goldstone bosons is capable of creating ordered patterns which would amount to self organization in the system.

The same argument applies to any other type of quasiparticle that may be present with significant scattering cross section with the reaction-diffusion particles and with large enough numbers such that a thermal bath of these quasiparticles exists. This line of reasoning leads to the possibility that $\dot{u}$ could account for all forms of dissipative scattering into any types of quasiparticles, not just phonons. If so, then the reaction-diffusion particles always become separated from their Goldstone bosons.

Photons would seem to be an exception to the rule. In many reaction-diffusion systems, recently created reaction products emit infrared photons and these typically leave the system. Thus, not all of the available stored energy will be available for creating the forces in the separation theorem. There are though, systems with short photon mean free paths, such as the hot plasmas, for example, found inside burning stars. In such systems the photons scatter frequently and become randomized to such an extent that they constitute their own heat bath. Under such conditions, photons and photon scattering may also adhere to the separation theorem. If so, then the separation theorem would hold with $\dot{u}$ being the total rate of dissipation arising from all possible processes. It remains to be shown that the result does indeed hold for reaction-diffusion particles scattering with photons since this would require a relativistic treatment. Logically, if $\dot{u}$ is the total rate of dissipation arising from all possible processes, including photons, then the result should then be called the strong form of the separation theorem.

V. EXAMPLE SYSTEM: SPATIAL GRADIENTS IN CATALYTIC SYSTEMS

For the previously studied electron-phonon system, a physical interface between two materials with different electrical conductivities provided an excellent example system for exhibiting a significant force on electrons, perpendicular to the interface, and an equal, and opposite, force on phonons. A chemical analogy would have the reaction transition probability varying spatially somehow. For a given reaction with

m reactants and n products, with the reaction transition probability represented by $\mathcal{R}$, consider the hypothetical scenario where all the particle concentrations and temperature are initially uniform but a nonzero gradient in the reaction transition probability exists, i.e., $\nabla\mathcal{R} \neq 0$. In a region with a larger than average value of $\mathcal{R}$, the rate $\dot{u}_R$ will be larger and the potential energy w_R will be lower. Reaction-diffusion particles will, overall, be pushed toward such a region and phonons will be pushed away.

One way to have $\mathcal{R}$ vary spatially is to introduce a catalyst. Wherever the catalyst is present, $\mathcal{R}$ is larger, thus creating a potential energy well at the location of the catalyst. This will enhance the catalytic effect. Since the catalyst already enhances the reaction rate, the physics introduced here provides a further enhancement. This makes the language challenging; the phrase *enhanced catalysis* is awkward yet may be apt. *Catalysis with active transport* also works.

The forces on some if not all of the reactants and products are uphill and therefore result in active transport. In this case it is primary active transport, whereby the active transport is driven by the release of stored chemical potential energy, i.e., by the ΔG of the reaction. In most discussions of active transport a biological membrane is present. Here it has been shown that primary active transport is possible in nonbiological systems and even in systems lacking a membrane. One role of such a membrane would be to allow for large concentrations inside the structure confined by the membrane, for example, a bacteria or a mitochondria. Also, for these small structures, chemical energy can be released at a high rate while maintaining a suitable operating temperature. On this point, the phonon force f_p will direct phonons to the exterior and this should help cool the structure. Thus, even though active transport can theoretically occur in nonbiological systems, biological systems may be best suited for creating significant examples of such transport.

A. Homogeneous catalysis and primary active transport

Before considering biological systems, some physical systems will be discussed. The first is an example of catalysis. A good example of homogeneous catalysis is acid catalysis in which there is a correlation between the reaction transition probability $\mathcal{R}$ and the pH of the system. One specific reaction is

$$CH_3CO_2CH_3 + H_2O \rightleftharpoons CH_3CO_2H + CH_3OH,$$
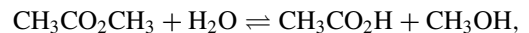
involving the hydrolysis of methyl acetate into acetic acid. The reaction-diffusion particles in this example are the reactants $CH_3CO_2CH_3$, H_2O, the products CH_3CO_2H, CH_3OH, as well as the catalyst $H+$. This reaction proceeds very slowly at neutral pH but proceeds rapidly under acidic conditions [43]. The analysis presented here predicts that if a pH gradient exists, then reactants and products will be pushed along the gradient lines toward lower pH regions.

To set up a simple calculation consider first a region of space which is pH neutral where $\dot{u}$ and w are both approximately zero. In a nearby region with low pH, the potential energy density $w = -\frac{1}{3}\tau^*\dot{u}$ [see Eqs. (82) and (95)] will be negative. Dividing w by the particle density gives a per parti-
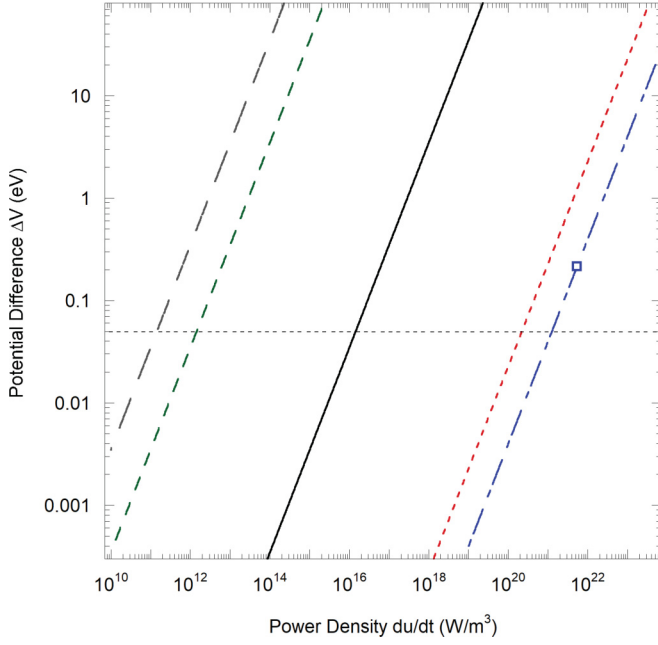
FIG. 5. Plots of calculated potential difference ΔV versus density of dissipated power. A particle concentration of 6.0×10^{23} m^{-3} was used for the solid (black) curve. At the 50 meV threshold (horizontal dashed line), $\dot{u} = 1.47 \times 10^{16}$ W/m^3. For the dot-dash (blue) curve, both the TNT particle density of $n_{rdp} = 4.39 \times 10^{27}$ m^{-3} and detonation velocity of 6900 m/s were used, and $\dot{u} = 1.27 \times 10^{21}$ W/m^3 at the 50 meV threshold. In comparison, for the short dash (red) curve the same density was used but with a smaller front velocity of 700 m/s. Here $\dot{u} = 2.22 \times 10^{20}$ W/m^3 at the 50 meV threshold. For the medium dash (green) curve $n_{rdp} = 6 \times 10^{19}$ m^{-3}, and $\dot{u} = 1.4 \times 10^{12}$ W/m^3 at the 50 meV threshold. Finally, for the long dash (gray) curve $n_{rdp} = 6 \times 10^{18}$ m^{-3}, and $\dot{u} = 1.4 \times 10^{11}$ W/m^3 at the 50 meV threshold. In all five plots, $\tau^* = 1$ ps was used.

cle potential energy difference:

$$-\Delta V \equiv \frac{w}{n_{rdp}}. \tag{101}$$

For a typical concentration of 0.001 mol/L (6×10^{23} m^{-3}), a plot of ΔV versus $\dot{u}$ is indicated in Fig. 5 as the solid (black) curve. A value of 1 ps is assumed for τ^*. From this curve, one needs a $\dot{u}$ value above 1×10^{14} W/m^3 before a chemical potential difference of even 1 meV is created. At lower power levels the potential difference predicted here is unlikely to be detected. Given that the phonon lifetime τ^* value is near 1 ps, the reaction in question would have to proceed very quickly before potential differences over a meV can be established. Reaction half lives would have to be near τ^* and half lives near 1 s and even near 1 ms give very small ΔV. Even half lives near 1 μs give small potential differences that would be difficult to detect.

By the same considerations, heterogeneous catalysis could also provide uphill active transport and perhaps be better at creating larger ΔV values. For a solid catalyst, it is the surface, i.e., the solid-gas or solid-liquid interface at which the catalytic activity occurs, and the potential energy well w is narrowly located at the interface. Away from the interface w is essentially zero. A complicating factor is that the energy well

in w could easily be confused with the significant potential energy well that is created by the chemisorption or physisorption processes at such interfaces.

With either type of catalysis, it is clear that very large power dissipation rate densities are needed to produce ΔV values near or above $k_B T$, where the effect becomes significant. For larger systems the heat load becomes problematic, creating an excessive temperature rise. For a sustained process, releasing energy quickly in structures at the nanometer scale is more plausible as heat can be dissipated away quickly enough. Otherwise, one can consider systems where the release of chemical potential energy energy is both brief and unbridled.

VI. EXAMPLE SYSTEM: EXPLOSIVE REACTIONS

Solid explosives may be characterized as having high density of stored chemical energy as well as high detonation velocities. Energy is released rapidly while high temperatures are attained. Trinitrotoluene (TNT) is a good example, with each molecule containing three high-energy $N \equiv N$ triple bonds and a detonation velocity v_d of 6900 m/s [44]. As the combustion front moves the reaction timescale can be as small as $n_{rdp}^{-1/3} \times v_d^{-1}$ which takes a value for τ_{rdp} of 0.09 ps for TNT. Making use of the cutoff time implemented in Eq. (60), as well as $\tau^* = 1$ ps, the cutoff time $\tilde{\tau} = 0.083$ ps. Equation (101) becomes

$$\Delta V \equiv -\frac{w}{n_{rdp}} = \frac{\tilde{\tau}\,\dot{u}}{3 n_{rdp}}, \tag{102}$$

which is used to add the (blue) dot-dash curve to Fig. 5.

With $E_0 = 34$ eV of energy per molecule of TNT, $\dot{u} = 5.0 \times 10^{21}$ Wm^{-3}, which is represented as the open square lying on the curve. The corresponding potential difference is $\Delta V = 0.197$ eV. At 197 meV of potential energy the effect would be to significantly push the molecules toward regions of higher density and constitutes another example of active transport in physical systems. Along the direction of the propagating explosion front this effect is still small compared to the pressure wave. However, significant transverse forces and velocities can exist if there are any density gradients along the front. Such gradients are expected in any real explosion; even if the system is designed with high symmetry, there will always exist small density gradients to begin with, and these will be enhanced by active transport.

By Eq. (49), a net impulse can be delivered to reaction-diffusion particles that depends on how strong this gradient α is. In this context it is understood that the final velocity v_f discussed here is the reaction-diffusion particle center of mass net velocity. The (green) short-dashed curve in Fig. 6 represents the monotonic relationship between the transverse final velocity v_f and the pre-reaction stored chemical energy A_0, with a small gradient $\alpha = 3 \times 10^5$ m^{-1}. With a specific $A_0 = E_0$ value for TNT, v_f takes a value of 1.5 m/s. The direction of this velocity is perpendicular to the front velocity vector v_d, and toward the larger concentration of reactants and products, i.e., in the direction opposite to diffusion. Larger gradients produce larger final velocities as indicated by the (red) dashed curve in Fig. 6 with a modest gradient of $\alpha = 1 \times 10^7$ m^{-1}.
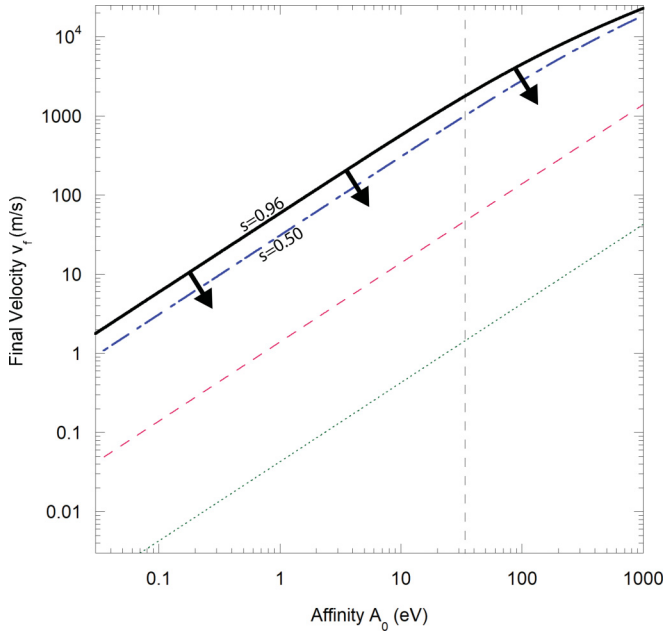
FIG. 6. Plots of calculated transverse boosted velocities versus reaction affinity. The solid (black) curve is calculated at a gradient parameter of $\alpha = 1.0 \times 10^{10}$ m^{-1}, which gives an s value close to the maximum value of unity. The dot-dash (blue) curve is calculated at $\alpha = 4.35 \times 10^{8}$ m^{-1}, while the long-dash (red) curve is calculated at $\alpha = 1.0 \times 10^{7}$ m^{-1}, and the short-dash (green) curve is calculated at $\alpha = 3.0 \times 10^{5}$ m^{-1}. Also indicated is the dashed vertical line at 34 eV, the stored energy value for a molecule of TNT.

The second law barrier, as described in Sec. II G 1 for the case where phonon energy can be extracted as useful work, represented here as $s = 0.5$, is indicated by the (blue) dot-dash curve at $\alpha = 4.35 \times 10^{8}$ m^{-1}. From this curve, a final velocity v_f of 1010 m/s is predicted at the same A_0 for TNT. Though not as high as the detonation velocity, this velocity still is very significant since it applies to particle motion transverse to the propagation direction of the front.

The final curve (black solid) in Fig. 6 is calculated at the relatively large value of $\alpha = 1.0 \times 10^{10}$ m^{-1}. Theoretically this is near the maximum allowed value when $s = 1$, according to the discussion in Sec. II G.

This example is important as it demonstrates that the forces calculated here can indeed become significant. Fast camera techniques could observe such active transport during explosions. Similar techniques used in the infrared could be used to observe temperature patterns and look for any abnormal heat flow as evidence of active phonon transport.

Also emphasized is the idea that a large power density is needed before these forces attain significant levels. In this case the large power density arises from the burning of chemical fuel at a high rate. At the propagating denotation front, very high values of $\dot{u}$ are attained, though briefly.

A related question is whether or not there exists any system that can produce significant forces f_{rdp} and potentials w_R over sustained periods of time, i.e., with large rates of fuel burning but without an explosion. This could happen with burn fronts moving at smaller velocities. It can also happen with smaller concentrations. The (red) short dash curve in Fig. 5 is the same

as the TNT case but with a smaller front velocity of 700 m/s. This shows that the same potential difference can be created at smaller power density. For example, the 50 meV threshold can be achieved at $\dot{u} = 2.22 \times 10^{20}$ W/m^3.

A clear picture emerges; in liquids and solids where τ^* is near 1 ps and particle densities are around 10^{27} m^{-3}, it is difficult to obtain 50 meV of potential energy difference unless the rate $\dot{u}$ is very large, indeed so large that the system is likely to be explosive. One way to avoid the explosion scenario is to invoke the bottlenecking effect discussed in Sec. III A 6. If a component B is sparse, such that n_B is relatively small, then these particles will experience a potential energy given to a good approximation by

$$\Delta V_B \equiv -\frac{w}{n_B} = \frac{\tau^* \dot{u}}{3 n_B}. \tag{103}$$

In biological systems, good candidates for the B component are small ions such as H$^+$, Na$^+$, and K$^+$.

VII. EXAMPLE SYSTEMS: PRIMARY ACTIVE TRANSPORT THROUGH A BIOLOGICAL SEMIPERMEABLE MEMBRANE

Biological systems such as bacteria and mitochondria could provide ideal conditions to drive processes that release energy at high power density, but without being explosive. The small size allows heat to be conducted away efficiently, while the semipermeable membrane allows for the creation of large concentration differences between the inside and outside. For many biological systems a membrane potential of about 50 meV is universally measured for ions such as H$^+$, Na$^+$, and K$^+$, capable of passing through the membrane. The results presented here show that such a potential is possible, but the $\dot{u}$ levels must be high. Glucose has a high-energy density, 77% as high as TNT, and given that it is consumed inside bacteria and mitochondria, the potential for creating significant forces f_{rdp} and f_p exists, if the rate of glycolysis is sufficiently high.

The argument for spatial gradients is the same as for the example of homogeneous catalysis in Sec. V. For example, as long as $\dot{u}$ is significant inside the mitochondrial matrix, then the gradient in $\dot{u}$ exists because the rate of glycolysis is low outside. The gradient will be greatest inside and near the transport channels of the semipermeable membrane.

If the rate $\dot{u}$ is indeed high enough, then all involved reaction-diffusion particles, i.e., reactants, products, and catalysts, could, in principle, build up a potential difference near 50 meV. The list of such particles is quite long, given the multistep complexity of the Krebs cycle, for instance.

A. Proton pumping in mitochondria during glycolysis

Many of the reaction-diffusion particles cannot pass through the semipermeable membrane of the mitochondria. Smaller particles such as protons can pass. As shown in Sec. III A 5, for a given reaction, a significant fraction of the released energy E_0 can go toward pumping protons uphill. Thus, protons can be pumped uphill up to a proton potential of possibly 50 meV, as long as protons play an important role in glycolysis.

A specific reaction that is an important step in the citric acid cycle that also involves protons is the decomposition of nicotinamide adenine dinucleotide:

$$NADH \rightleftharpoons NAD + H + 2e-.$$

This reaction is an good example of how a significant fraction of any released energy can go toward proton pumping. Indeed, this reaction is known to push protons outside of the mitochondrial matrix as an example of primary active transport [5].

On the issue of how much energy must be released, the medium-dash (green) curve in Fig. 5 shows the relation indicated in Eq. (103) at a H$^+$ concentration of $n_B = 6 \times 10^{19}$ m^{-3}, i.e., at a pH of 7.0. Also shown by the long dash (gray) curve is the same relation at a pH of 8.0, which is close to conditions inside the mitochondrial matrix. At a pH of 8.0, the 50 meV threshold occurs at a power level of $\dot{u} = 1.4 \times 10^{11}$ W/m^3.

There are other steps in the citric acid cycle that also actively transport protons to the exterior, so this one reaction does not need to produce the entire 50 mV of potential. The calculations developed here do show that the measured potential difference of protons can be produced if power levels are near 10^{11} W/m^3. Since this is about eleven orders of magnitude lower than for the explosive TNT reaction, such sustained power levels should not lead to irreparable physical damage. If mitochondria do indeed burn glucose near this rate, then this makes f_{rdp} a good candidate for explaining the physical mechanism for primary active transport in mitochondria. For active transport of ions there is an electrostatic force that must be overcome. This external force was represented by $\boldsymbol{F}_{ext}$ in Eq. (1). If the second-order force discussed here can overcome this external force, then active ion transport is possible.

The pumping process for a given proton can be very quick, while $\dot{u}$ is very large. Given that 50 mV of proton potential inside a small structure such as a mitochondria only requires a small number of protons (≈ 10), one realizes that $\dot{u}$ does not need to be large all of the time. There can be short bursts of time where $\dot{u}$ is large and proton pumping is active, followed by longer periods of time where $\dot{u}$ is small and the mitochondrial membrane seals itself off. The enzyme protein ATP synthase, located nearby the membrane channels may play a role in this alternating state of either allowing or blocking proton transport across the membrane, i.e., in controlling the duty cycle. Time averaging over such a duty cycle may give a power production density inside a mitochondria that is considerably smaller than the $\dot{u}$ values discussed here.

B. Photosynthesis example

Another example of note is photosynthesis in which a visible photon is absorbed at a chloroplast and exergonically converted into a proton membrane potential that can later provide the energy for ATP synthesis. The excitonic cascade at a cytochrome b$_6$f complex, immediately following the photonic excitation, occurs over a timescale of about 30 ps [5]. A significant portion of the photon energy is used to pump protons into the chloroplast. The potential energy stored in protonic electrochemical potential is used subsequently to create ATP. Again, this creates a plausible model with a few

eV of energy dissipated into a small volume over a short time. Large rates $\dot{u}$ are possible. Putting some numbers in for chlorophyll b, photons are absorbed at $E_0 = 2.7$ eV, at a pH of 7.0, $n_{proton} = 6 \times 10^{19}$ m^{-3}, and making use of the 30 ps timescale, i.e., $\tau_{rdp} = 30$ ps, then $\dot{u} = 8.6 \times 10^{11}$ W/m^3. By Eq. (103), $\Delta V_{proton} = 90$ meV, which is more than sufficient to establish the observed proton potential.

C. Directionality of active transport

In the two biological examples considered earlier in this section, transport theory including second-order scattering is capable of explaining active proton transport that is effective enough to produce an electrical potential of 50 mV.

For a first principles physical theory to explain active transport in biological membrane systems, the following four conditions must be satisfied: (1) As just discussed, energy must be released at both a high rate and at a high density. When $\dot{u}$ is large enough then potential differences in the range of 50 mV can be created across the membrane. (2) The second law of thermodynamics must not be violated. Calculations suggest e_{ex} is limited to no more than one-third. (3) The exergonic conversion factor e_{ex} must not be too small. From the analysis in Sec. III A 5, calculations for e_{ex} suggest it is close to the one-third limit, using reasonable estimates for the relevant parameters. Realistically the factor would need to be near this limiting value. If e_{ex} is too small, then too much energy must be expended by the organism for too little gain. A high spatial gradient α is essential to this, and again the membrane plays an important role. (4) The active transport must be highly directional, and of course, in the right direction. For active proton transport in particular, no clear physical explanation exists for the directionality of this motion. The availability of energy does not guarantee that any ions can be pushed uphill energetically. There are indeed many chemical reactions that release energy while not being known for any type of active transport, self assembly, or pattern formation. Something else is needed besides the energy; the actively transported particles must be directed uphill.

For the photosynthesis example discussed in Sec. VII B, the calculated force $\boldsymbol{f}_{rdp}$ which is always in the same direction as the gradient in $\tau^*\dot{u}$, will point point inwards, i.e., to draw particles from the outside to the inside of the chloroplast. This is indeed what is observed for protons in such systems during photosynthesis, i.e., protons are actively pumped into the chloroplast.

As encouraging as these calculations are that $\boldsymbol{f}_{rdp}$ does indeed play an important role in biological transport processes, the complete picture still awaits and there is more work to be done. For example, for the glycolysis example discussed in Sec. VII A, the equations predict $\boldsymbol{f}_{rdp}$ to point inwards, because $\dot{u}$ is larger inside, and yet the protons are pushed outwards. They are pushed uphill, energetically, but a detailed explanation is lacking for why $\boldsymbol{f}_B$ points opposite to $\boldsymbol{f}_{rdp}$. The situation is quite simple when there is only one type of reaction-diffusion particle; the force on that particle is $\boldsymbol{f}_{rdp}$ and the direction at any point in space is determined by the $\tau^*\dot{u}$ field. For multicomponent reactions such as glycolysis taking place inside of mitochondria, the $\tau^*\dot{u}$ field only determines the center-of-mass force $\boldsymbol{f}_{rdp}$. The proton force need not be

in the same direction as $\boldsymbol{f}_{\text{rdp}}$. In such systems, the magnitude of $\boldsymbol{f}_{\text{rdp}}$ should, at best, be considered a good estimate for the magnitude of the proton force. More accurate calculations for the proton force, as well as forces on other products and reactants, requires using Eqs. (92) and (93). The integrals in these force expressions would need to be evaluated numerically in any future work.

These expressions have great potential for calculating dynamics of all reactants and products, as well as heat flow, to great detail. Many examples of proton pumping involve the well studied enzyme ATP synthase. This is a large protein complex (≈ 500 kDa) some of which is embedded in a membrane. The enzyme facilitates proton transfer across the membrane in both the energetically downhill and uphill directions. Moreover, the proton transfer is coupled to mechanical rotation of large subunits of the ATP synthase, for example the F_0 rotor [45,46]. This rotation orientation is also coupled to the catalysis of ATP in both directions, synthesis and hydrolysis.

The formalism developed here, Eqs. (92) and (93), may be capable of providing a detailed explanation of this enzyme's dynamics, including the rotation and any uphill active transport. This formalism does allow for forces, and therefore torques, all calculated at second order, to be exerted on any participating reaction-diffusion particles, including protons, ADP, ATP, and the various components making up the enzyme. These are forces and torques that cannot be accounted for by first-order, linear, transport theory.

VIII. CONCLUSIONS

For reaction-diffusion systems, a Boltzmann transport equation is formulated which accounts for collisions up to second order. Reactants and products scatter with phonons for first order and this is combined with three-phonon scattering for the second order to produce the reaction-diffusion-phonon Boltzmann transport equation. All possible types of reactions have been considered, including combination and bimolecular reactions.

Two forces are produced in general which push all reactants, products, and catalysts together in one direction while the phonons are pushed in the opposite direction. Momentum is conserved. Because of these forces, exergonic conversion

is possible, i.e., not all of the released energy becomes heat. Spatial gradients play an important role. This includes gradients in particle concentrations, temperature, and scattering strength for both reaction-diffusion particle-phonon scattering as well as phonon-phonon scattering. In cases where the reactive cross section varies spatially, the reaction-diffusion particles are pushed toward regions of higher catalytic activity.

These forces are simply expressed in terms of the gradient of the product of the phonon lifetime and the rate of dissipation. When strong gradients are combined with fast energy release the forces can be significant. Numerical calculations show this to be the case during explosive reactions. Similar calculations at lower power demonstrate the possibility that these forces are responsible for active proton transport across semipermeable biological membranes. While obeying the second law, up to one-third of the available chemical energy is converted by ion pumping to create sufficient electric potential energy for Mitchell's chemiosmotic theory to be workable.

The analysis shows that phonon transport plays an important role in reaction-diffusion systems. The phonon force can produce instability in the temperature field which in turn can produce Turing patterns. Indeed, the separating force pair can exist, even if the temperature and all concentrations are uniform.

Given that the spatial gradients discussed here realistically exist in all nonequilibrium systems, the forces predicted to separate reaction-diffusion particles from phonons should play some role in all reaction-diffusion systems. Indeed, given these forces have been also predicted in the electron-phonon system, it would seem that the forces may exist in all nonequilibrium systems.

The forces are unexpected, as they do not exist in thermodynamic equilibrium. One can characterize these forces as emergent, i.e., these forces contribute to emergent behavior such as Turing pattern formation. The analysis presented here also clearly shows how such emergent and complex behavior can be reduced down to the fundamental and simple forces of physics.

APPENDIX A: NEAR EQUILIBRIUM EXPANSION FOR DIFFUSION

Even with the focus away from near equilibrium it is still instructive to show the standard near equilibrium expansion for $g_{\boldsymbol{k}}$. One begins with the equilibrium distribution,

$$g_{\boldsymbol{k}}^0 = e^{-\beta(E_k - \mu)} = \frac{1}{Z} e^{-\beta E_k}, \tag{A1}$$

with $E_k = \frac{\hbar^2}{2m} k^2$. For the nonequilibrium reaction-diffusion particle distribution one shifts the wave vector by a small amount $k_0 \hat{\boldsymbol{z}}$:

$$\tilde{E}_k = \frac{\hbar^2}{2m}(\boldsymbol{k} - k_0\hat{\boldsymbol{z}})^2 \approx E_k + \frac{\hbar^2}{2m}k_0^2 - \frac{\hbar^2}{m}k_0 k_z. \tag{A2}$$

To a good approximation

$$\frac{g_{\boldsymbol{k}}}{g_{\boldsymbol{k}}^0} = \left\{ 1 + \frac{\beta\hbar^2 k_z k_0}{m} - \beta K\left[1 - \frac{\beta\hbar^2 k_z^2}{m} \right] \right\}, \tag{A3}$$

where the kinetic energy

$$K \equiv \frac{\hbar^2 k_0^2}{2m}.$$ (A4)

Thus, the difference:

$$\frac{g_k}{g_k^0} - e^{-\beta \varepsilon_{q''}} \frac{g_{k'}}{g_k^0} = \frac{\beta \hbar^2 k_0}{m}(k_z - k_z') + \xi \frac{\beta \hbar^2}{m}[k_z^2 - (k_z')^2].$$ (A5)

When inserted into Eq. (10) the result is

$$\dot{u}_{ph} = \frac{\beta^2 \hbar^2 K}{m} \iiint g_k^0 (1 + h_{q''}^0) \mathcal{W}_k^{k',q''} \delta(\mathbf{k} - \mathbf{k'} - \mathbf{q''})[k_z^2 - (k_z')^2]\varepsilon_{q''} d\mathbf{k} d\mathbf{k'} d\mathbf{q''}.$$ (A6)

By symmetry this must be same as if $k_z^2 - (k_z')^2$ is replaced by $k_x^2 - (k_x')^2$ or $k_y^2 - (k_y')^2$ or $\frac{1}{3}[k^2 - (k')^2]$. Since $E_k = E_{k'} + \varepsilon_{q''}$:

$$\dot{u}_{ph} = \frac{2}{3}\beta^2 K \iiint g_k^0 (1 + h_{q''}^0) \mathcal{W}_k^{k',q''} \delta(\mathbf{k} - \mathbf{k'} - \mathbf{q''})\varepsilon_{q''}^2 d\mathbf{k} d\mathbf{k'} d\mathbf{q''}.$$ (A7)

Here one sees directly that the force is proportional to k_0^2 which is proportional to $|\nabla n_c|^2$.

APPENDIX B: VERIFICATION OF PHONON FORCE FOR COMBINATION REACTIONS

For phonon wave vector $\mathbf{q}$ the second-order collision integral analogous to Eq. (70) is

$$\begin{aligned}
\frac{\partial h_q}{\partial t}\Big|_{R2} = \int_0^\infty \iiiint \Big[& \{-e^{-t'/\tau_{1,>}} g_A g_B h_q (1 + h_{q'}) + e^{-t'/\tau_{1,<}} g_C (1 + h_q) h_{q'}\} \mathcal{Q}_{q'',q}^{q'} \delta(\mathbf{q''} + \mathbf{q} - \mathbf{q'}) \\
& + \{e^{-t'/\tau_{2,>}} g_A g_B (1 + h_q)(1 + h_{q'}) - e^{-t'/\tau_{2,<}} g_C h_q h_{q'}\} \mathcal{Q}_{q''}^{q,q'} \delta(\mathbf{q''} - \mathbf{q} - \mathbf{q'}) \Big] \\
& \times (1 + n_{q''}) n_{q''} \mathcal{R}_{A,B}^{C,q''} \delta(\mathbf{k}_A + \mathbf{k}_B - \mathbf{k}_C - \mathbf{q''}) d\mathbf{k}_A d\mathbf{k}_B d\mathbf{k}_C d\mathbf{q'} d\mathbf{q''} dt'.
\end{aligned}$$ (B1)

Similarly, for $\mathbf{q'}$,

$$\begin{aligned}
\frac{\partial h_{q'}}{\partial t}\Big|_{R2} = \int_0^\infty \iiiint \Big[& \{e^{-t'/\tau_{1,>}} g_A g_B h_q (1 + h_{q'}) - e^{-t'/\tau_{1,<}} g_C (1 + h_q) h_{q'}\} \mathcal{Q}_{q'',q}^{q'} \delta(\mathbf{q''} + \mathbf{q} - \mathbf{q'}) \\
& + \{e^{-t'/\tau_{2,>}} g_A g_B (1 + h_q)(1 + h_{q'}) - e^{-t'/\tau_{2,<}} g_C h_q h_{q'}\} \mathcal{Q}_{q''}^{q,q'} \delta(\mathbf{q''} - \mathbf{q} - \mathbf{q'}) \Big] \\
& \times (1 + h_{q''}) h_{q''} \mathcal{R}_{A,B}^{C,q''} \delta(\mathbf{k}_A + \mathbf{k}_B - \mathbf{k}_C - \mathbf{q''}) d\mathbf{k}_A d\mathbf{k}_B d\mathbf{k}_C d\mathbf{q} d\mathbf{q''} dt'.
\end{aligned}$$ (B2)

The phonon force is

$$f_{p,R} = \frac{1}{2}\hbar \int \mathbf{q} \frac{\partial h_q}{\partial t}\Big|_{R2} d\mathbf{q} + \frac{1}{2}\hbar \int \mathbf{q'} \frac{\partial h_{q'}}{\partial t}\Big|_{R2} d\mathbf{q'}.$$ (B3)

Explicitly,

$$\begin{aligned}
f_{p,R} = \frac{1}{2}\hbar \int_0^\infty \iiiint \Big[& \{-e^{-t'/\tau_{1,>}} g_A g_B h_q (1 + h_{q'}) + e^{-t'/\tau_{1,<}} g_C (1 + h_q) h_{q'}\} \mathcal{Q}_{q'',q}^{q'} \delta(\mathbf{q''} + \mathbf{q} - \mathbf{q'})\mathbf{q} \\
& + \{e^{-t'/\tau_{2,>}} g_A g_B (1 + h_q)(1 + h_{q'}) - e^{-t'/\tau_{2,<}} g_C h_q h_{q'}\} \mathcal{Q}_{q''}^{q,q'} \delta(\mathbf{q''} - \mathbf{q} - \mathbf{q'})\mathbf{q} \Big] \\
& \times (1 + h_{q''}) h_{q''} \mathcal{R}_{A,B}^{C,q''} \delta(\mathbf{k}_A + \mathbf{k}_B - \mathbf{k}_C - \mathbf{q''}) d\mathbf{k}_A d\mathbf{k}_B d\mathbf{k}_C d\mathbf{q} d\mathbf{q'} d\mathbf{q''} dt' \\
+ \frac{1}{2}\hbar \int_0^\infty \iiiint \Big[& \{e^{-t'/\tau_{1,>}} g_A g_B h_q (1 + h_{q'}) - e^{-t'/\tau_{1,<}} g_C (1 + h_q) h_{q'}\} \mathcal{Q}_{q'',q}^{q'} \delta(\mathbf{q''} + \mathbf{q} - \mathbf{q'})\mathbf{q'} \\
& + \{e^{-t'/\tau_{2,>}} g_A g_B (1 + h_q)(1 + h_{q'}) - e^{-t'/\tau_{2,<}} g_C h_q h_{q'}\} \mathcal{Q}_{q''}^{q,q'} \delta(\mathbf{q''} - \mathbf{q} - \mathbf{q'})\mathbf{q'} \Big] \\
& \times (1 + h_{q''}) h_{q''} \mathcal{R}_{A,B}^{C,q''} \delta(\mathbf{k}_A + \mathbf{k}_B - \mathbf{k}_C - \mathbf{q''}) d\mathbf{k}_A d\mathbf{k}_B d\mathbf{k}_C d\mathbf{q} d\mathbf{q'} d\mathbf{q''} dt'.
\end{aligned}$$ (B4)

Regrouping gives

$$\begin{aligned}
f_{p,R} = \frac{1}{2}\hbar \int_0^\infty \iiiint \Big[& \{e^{-t'/\tau_{1,>}} g_A g_B h_q (1 + h_{q'}) - e^{-t'/\tau_{1,<}} g_C (1 + h_q) h_{q'}\} \mathcal{Q}_{q'',q}^{q'} \delta(\mathbf{q''} + \mathbf{q} - \mathbf{q'})\mathbf{q''} \\
& + \{e^{-t'/\tau_{2,>}} g_A g_B (1 + h_q)(1 + h_{q'}) - e^{-t'/\tau_{2,<}} g_C h_q h_{q'}\} \mathcal{Q}_{q''}^{q,q'} \delta(\mathbf{q''} - \mathbf{q} - \mathbf{q'})\mathbf{q''} \Big] \\
& \times (1 + h_{q''}) h_{q''} \mathcal{R}_{A,B}^{C,q''} \delta(\mathbf{k}_A + \mathbf{k}_B - \mathbf{k}_C - \mathbf{q''}) d\mathbf{k}_A d\mathbf{k}_B d\mathbf{k}_C d\mathbf{q} d\mathbf{q'} d\mathbf{q''} dt'.
\end{aligned}$$ (B5)

Making use of Eqs. (14), (15), (16), and (17) in Eq. (B5) allows simplification to

$$
f_{p,R} = \hbar \int_0^\infty \iiiint \left[\left\{ e^{-t'/\tau_{1,>}} g_A g_B (1 + h_{q''}) \frac{1}{\tau'_{1,>}} - e^{-t'/\tau_{1,<}} g_C h_{q''} \frac{1}{\tau'_{1,<}} \right\} q'' \right.
$$
$$
\left. + \left\{ e^{-t'/\tau_{2,>}} g_A g_B (1 + h_{q''}) \frac{1}{\tau'_{2,>}} - e^{-t'/\tau_{2,<}} g_C h_{q''} \frac{1}{\tau'_{2,<}} \right\} q'' \right] \mathcal{R}_{A,B}^{C,q''} \delta(\boldsymbol{k}_A + \boldsymbol{k}_B - \boldsymbol{k}_C - \boldsymbol{q''}) d\boldsymbol{k}_A d\boldsymbol{k}_B d\boldsymbol{k}_C d\boldsymbol{q''} dt'. \quad \text{(B6)}
$$

Dropping the two reverse flow terms gives

$$
f_{p,R} = \hbar \int_0^\infty \iiiint \boldsymbol{q''} \left[e^{-t'/\tau_{1,>}} g_A g_B (1 + h_{q''}) \frac{1}{\tau'_{1,>}} + e^{-t'/\tau_{2,>}} g_A g_B (1 + h_{q''}) \frac{1}{\tau'_{2,>}} \right] \mathcal{R}_{A,B}^{C,q''}
$$
$$
\times \delta(\boldsymbol{k}_A + \boldsymbol{k}_B - \boldsymbol{k}_C - \boldsymbol{q''}) d\boldsymbol{k}_A d\boldsymbol{k}_B d\boldsymbol{k}_C d\boldsymbol{q''} dt'. \quad \text{(B7)}
$$

Comparing to Eq. (77) one verifies that $f_p = -f_{\text{rdp},R}$.

APPENDIX C: NEAR EQUILIBRIUM EXPANSION FOR DIFFUSION AND COMBINATION REACTION

If a concentration gradient in reactant A created during the combination reaction $A + B \leftrightarrow C + p$, then a subsequent number current density J_A is produced. The transport analysis is similar to that in Appendix A [see Eq. (A7)] with the following result:

$$
\dot{u}_{p,A} = \frac{2}{3} \beta^2 K_A \iiiint g_A^0 g_B^0 (1 + h_{q''}^0) \mathcal{R}_{A,B}^{C,q''} \delta(\boldsymbol{k}_A + \boldsymbol{k}_B - \boldsymbol{k}_C - \boldsymbol{q''}) \varepsilon_{q''}^2 d\boldsymbol{k}_A d\boldsymbol{k}_B d\boldsymbol{k}_C d\boldsymbol{q''}, \quad \text{(C1)}
$$

where

$$
K_A = \frac{m_A J_A^2}{2 n_A^2}. \quad \text{(C2)}
$$

The analysis is similar for reactant B and product C, giving the additive factors, $K_B = \frac{m_B J_B^2}{2 n_B^2}$ and $K_C = \frac{m_C J_C^2}{2 n_C^2}$. Adding the three terms gives Eq. (C1) with K_A replaced by $K_A + K + B + K_C$.

Reactions are distinguished from diffusion when noting that even with reactant and product densities uniform, there can be a nonzero affinity. De Donder's affinity is defined as

$$
A = \Delta \mu_A + \Delta \mu_B - \Delta \mu_C. \quad \text{(C3)}
$$

Referring to Eq. (68):

$$
g_A g_B (1 + h_{q''}) - g_C h_{q''} = \left[g_A^0 g_B^0 (1 + h_{q''}^0) e^{\beta(\Delta\mu_A + \Delta\mu_B)} - g_C^0 h_{q''}^0 e^{\beta\Delta\mu_C} \right], \quad \text{(C4)}
$$

$$
g_A g_B (1 + h_{q''}) - g_C h_{q''} = e^{\beta\Delta\mu_C} \left[g_A^0 g_B^0 (1 + h_{q''}^0) e^{\beta(\Delta\mu_A + \Delta\mu_B - \Delta\mu_C)} - g_C^0 h_{q''}^0 \right], \quad \text{(C5)}
$$

$$
g_A g_B (1 + h_{q''}) - g_C h_{q''} \approx \left[g_A^0 g_B^0 (1 + h_{q''}^0) e^{\beta(\Delta\mu_A + \Delta\mu_B - \Delta\mu_C)} - g_C^0 h_{q''}^0 \right], \quad \text{(C6)}
$$

$$
g_A g_B (1 + h_{q''}) - g_C h_{q''} \approx \left[g_A^0 g_B^0 (1 + h_{q''}^0) - g_C^0 h_{q''}^0 \right] + \beta A g_A^0 g_B^0 (1 + h_{q''}^0), \quad \text{(C7)}
$$

$$
g_A g_B (1 + h_{q''}) - g_C h_{q''} \approx \beta A g_A^0 g_B^0 (1 + h_{q''}^0), \quad \text{(C8)}
$$

$$
\dot{u}_{\text{reaction}} = \beta A \iiiint g_A^0 g_B^0 (1 + h_{q''}^0) \mathcal{R}_{A,B}^{C,q''} \delta(\boldsymbol{k}_A + \boldsymbol{k}_B - \boldsymbol{k}_C - \boldsymbol{q''}) \varepsilon_{q''} d\boldsymbol{k}_A d\boldsymbol{k}_B d\boldsymbol{k}_C d\boldsymbol{q''}. \quad \text{(C9)}
$$

Note there is one less factor of $\varepsilon_{q''}$ as compared to Eq. (C1). For exothermic combination reactions, $A > 0$ and $\dot{u}_{\text{reaction}}$ is positive. The net power dissipation is

$$
\dot{u}_{p,R} = \dot{u}_{p,A} + \dot{u}_{p,B} + \dot{u}_{p,C} + \dot{u}_{\text{reaction}}. \quad \text{(C10)}
$$

[1] S. N. Patitsas, Electronic transport calculations showing electron-phonon separation in directions transverse to high current, J. Phys. Commun. **5**, 095007 (2021).

[2] A. M. Turing, The chemical basis of morphogenesis, Philos. Trans. R. Soc. London B **237**, 37 (1952).

[3] M. C. Cross and P. C. Hohenberg, Pattern formation outside of equilibrium, Rev. Mod. Phys. **65**, 851 (1993).

[4] P. Mitchell, Coupling of phosphorylation to electron and hydrogen transfer by a chemi-osmotic type of mechanism, Nature (London) **191**, 144 (1961).

[5] D. L. Nelson and M. M. Cox, *Lehninger Principles of Biochemistry* (Macmillan, New York, NY, 2021).

[6] J. Ziman, *Electrons and Phonons* (Oxford University Press, Oxford, UK, 1960).

[7] N. W. Ashcroft and D. N. Mermin, *Solid State Physics*, 1st ed. (Saunders College, Philadelphia, PA, 1976).

[8] J. Ross and P. Mazur, Some deductions from a formal statistical mechanical theory of chemical kinetics, J. Chem. Phys. **35**, 19 (1961).

[9] B. Shizgal and M. Karplus, Nonequilibrium contributions to the rate of reaction. I. Perturbation of the velocity distribution function, J. Chem. Phys. **52**, 4262 (1970).

[10] B. Shizgal and M. Karplus, Nonequilibrium contributions to the rate of reactions. II. Isolated multicomponent systems, J. Chem. Phys. **54**, 4345 (1971).

[11] B. Shizgal and M. Karplus, Nonequilibrium contribution to the rate of reaction. III. Isothermal multicomponent systems, J. Chem. Phys. **54**, 4357 (1971).

[12] F. Baras and M. M. Mansour, Validity of Macroscopic Rate Equations in Exothermic Chemical Systems, Phys. Rev. Lett. **63**, 2429 (1989).

[13] H. Kreuzer, *Nonequilibrium Thermodynamics and its Statistical Foundations* (Clarendon Press, Oxfrod, UK, 1981).

[14] J. A. Sussmann and A. Thellung, Thermal conductivity of perfect dielectric crystals in the absence of Umklapp processes, Proc. Phys. Soc. **81**, 1122 (1963).

[15] R. A. Guyer and J. A. Krumhansl, Solution of the linearized phonon Boltzmann equation, Phys. Rev. **148**, 766 (1966).

[16] H. E. Jackson and C. T. Walker, Thermal conductivity, second sound, and phonon-phonon interactions in NaF, Phys. Rev. B **3**, 1428 (1971).

[17] G. Srivastava, *The Physics of Phonons* (Adam Hilger, New York, NY, 1990).

[18] S. Chapman and T. Cowling, *The Mathematical Theory of Non-uniform Gases* (Cambridge University Press, Cambridge, UK, 1970).

[19] F. Reif, *Fundamentals of Statistical and Thermal Physics* (McGraw Hill, New York, NY, 1965).

[20] J. M. Luttinger, An exactly soluble model of a many-fermion system, J. Math. Phys. **4**, 1154 (1963).

[21] F. D. M. Haldane, Luttinger liquid theory of one-dimensional quantum fluids. I. Properties of the Luttinger model and their extension to the general 1D interacting spinless Fermi gas, J. Phys. C **14**, 2585 (1981).

[22] C. Kim, A. Y. Matsuura, Z.-X. Shen, N. Motoyama, H. Eisaki, S. Uchida, T. Tohyama, and S. Maekawa, Observation of Spin-Charge Separation in One-Dimensional $SrCuO_2$, Phys. Rev. Lett. **77**, 4054 (1996).

[23] N. G. van Kampen, Thermal fluctuations in a nonlinear system, Phys. Rev. **110**, 319 (1958).

[24] M. Simoncelli, N. Marzari, and F. Mauri, Unified theory of thermal transport in crystals and glasses, Nat. Phys. **15**, 809 (2019).

[25] J. A. Krumhansl, Thermal conductivity of insulating crystals in the presence of normal processes, Proc. Phys. Soc. **85**, 921 (1965).

[26] D. D. Joseph and L. Preziosi, Heat waves, Rev. Mod. Phys. **61**, 41 (1989).

[27] Y. Kuramoto and T. Tsuzuki, Persistent propagation of concentration waves in dissipative media far from thermal equilibrium, Prog. Theor. Phys. **55**, 356 (1976).

[28] G. Sivashinsky, Nonlinear analysis of hydrodynamic instability in laminar flames I. Derivation of basic equations, Acta Astronaut. **4**, 1177 (1977).

[29] D. Michelson, Steady solutions of the Kuramoto-Sivashinsky equation, Physica D **19**, 89 (1986).

[30] P. Manneville, *The Kuramoto-Sivashinsky Equation: A Progress Report* (Springer, Berlin, 1988), pp. 265–280.

[31] R. C. Desai and R. Kapral, *Dynamics of Self-organized and Self-Assembled Structures* (Cambridge, New York, NY, 2009).

[32] M. Cross and H. Greenside, *Pattern Formation and Dynamics in Nonequilibrium Systems* (Cambridge, New York, NY, 2009).

[33] S. N. Patitsas, Nonequilibrium phase transitions and pattern formation as consequences of second-order thermodynamic induction, Phys. Rev. E **100**, 022116 (2019).

[34] V. Castets, E. Dulos, J. Boissonade, and P. De Kepper, Experimental Evidence of a Sustained Standing Turing-Type Nonequilibrium Chemical Pattern, Phys. Rev. Lett. **64**, 2953 (1990).

[35] Q. Ouyang and H. L. Swinney, Transition from a uniform state to hexagonal and striped Turing patterns, Nature (London) **352**, 610 (1991).

[36] Q. Ouyang and H. L. Swinney, Transition to chemical turbulence, Chaos **1**, 411 (1991).

[37] A. M. Zhabotinsky, A history of chemical oscillations and waves, Chaos **1**, 379 (1991).

[38] Q. Ouyang, Z. Noszticzius, and H. L. Swinney, Spatial bistability of two-dimensional Turing patterns in a reaction-diffusion system, J. Phys. Chem. **96**, 6773 (1992).

[39] V. K. Vanag and I. R. Epstein, Pattern Formation in a Tunable Medium: The Belousov-Zhabotinsky Reaction in an Aerosol Or Microemulsion, Phys. Rev. Lett. **87**, 228301 (2001).

[40] R. Zwanzig, Diffusion past an entropy barrier, J. Phys. Chem. **96**, 3926 (1992).

[41] D. Reguera and J. M. Rubí, Kinetic equations for diffusion in the presence of entropic barriers, Phys. Rev. E **64**, 061106 (2001).

[42] D. Reguera, G. Schmid, P. S. Burada, J. M. Rubí, P. Reimann, and P. Hänggi, Entropic Transport: Kinetics, Scaling, and Control Mechanisms, Phys. Rev. Lett. **96**, 130603 (2006).

[43] R. Bell, *The Proton in Chemistry*, George Fisher Baker non-resident lectureship in chemistry at Cornell University (Springer U.S., Boston, MA, 2013).

[44] W. Copper, Paul, *Explosives Engineering* (Wiley, New York, NY, 1996).

[45] D. Stock, C. Gibbons, I. Arechaga, A. G. Leslie, and J. E. Walker, The rotary mechanism of ATP synthase, Curr. Opin. Struct. Biol. **10**, 672 (2000).

[46] M. Yoshida, E. Muneyuki, and T. Hisabori, ATP synthase—A marvellous rotary engine of the cell, Nat. Rev. Mol. Cell Biol. **2**, 669 (2001).